Pressure of Partial Crystallization of Katla Magmas: Implications for Magma Chamber Depth and for the Magma Plumbing System

Research Thesis

Presented in partial fulfillment of the requirements for graduation with research distinction in Geological Sciences in the undergraduate colleges of The Ohio State University

By

Andrew J. Tenison

The Ohio State University

Project Advisor: Dr. Michael Barton, School of Earth Sciences

TABLE OF CONTENTS

Abstract

Iceland is home to some of the most active volcanoes in the world, and recent eruptions emphasize the need for additional studies to better understand the volcanism and tectonics in this region. Historical patterns of eruptive activity and an increase in seismic activity suggest that Katla is showing signs of an impending eruption. The last major eruption in 1918 caused massive flooding and deposited enough sediment to extend part of Iceland's southern shoreline by 5 km. It also generated sufficient ash over many weeks to cause a brief drop in global temperature. A future eruption similar to the 1918 event could have serious global consequences, including severe disruptions in air travel, short-term global cooling, and shortened growing seasons. Relatively few studies have focused on establishing the depth of the main magma chamber beneath Katla, although knowledge of magma chamber depth is essential for constraining models for magma evolution and for understanding the eruption dynamics of this volcano. The results of seismic and geodetic studies suggest the presence of a shallow magma body at a depth of 2-4 km, but do not provide firm evidence for the presence of deeper chambers in contrast to results obtained for other volcanoes in Iceland. Studies of volcanic ash layers reveal a history of alternating cycles of basaltic and silicic eruptions. I suggest that the shallow magma chamber is primarily the source of silica-rich magma, and postulate that there must be one or more additional chambers in the middle or deep crust that serve as the storage site of the basaltic magma erupted as lava and ash. I have tested this proposal by calculating the pressures of partial crystallization for basalts erupted at Katla using petrological methods. These pressures can be converted to depths and the results provide insight into the likely configuration of the magma plumbing system. Published analyses of volcanic glasses (lava, ash and hyaloclastite) were used as input data.

The raw data were filtered to remove non basalts and to exclude basalt samples with anomalous chemical compositions. Pressures of partial crystallization were calculated by quantitatively comparing the compositions of the glasses with those of experimental liquids in equilibrium with olivine, plagioclase, and augite at different pressures and temperatures using the approach described by Yang and co-workers (1996). The results for samples that yielded pressures associated with unrealistically large uncertainties were filtered out of the database. Pressures for the remaining samples were converted to depths assuming an average crustal density of 2900 kg/m^3. The results indicate that most magmas partially crystallized over a range of pressures corresponding to a range of depths from 20 to 25 km. I conclude that one or more magma chambers occur in this depth range, or at slightly shallower depths if the effects of water on calculated pressures of partial crystallization are taken into account. Most erupted basalts have ascended from this depth directly to the surface, presumably via dikes. The Katla plumbing system is thus similar to that at other major volcanoes (Hekla, Bardarbunga, Grímsvötn) in the eastern volcanic zone inasmuch as the majority of the erupted magmas are supplied from chambers in the middle and lower crust at depths of 10 to 30 km.

Acknowledgements

I would first like to thank my academic advisor Dr. Anne Carey for doing a terrific job in guiding my academic success. When I transferred out of engineering, she showed me that I still would be able to graduate in four years and laid out a clear plan for doing so. She has been instrumental in helping me secure research grants and scholarships from the university which allowed me to travel to Iceland to do field research. Without her guidance, I would not be the earth scientist I am today.

Without extensive funding, the incredible undergraduate research experiences I have had would not be possible. I want to thank the Shell Exploration and Production Company for funding research during the summer of 2011 which helped get this project off the ground. I also would like to acknowledge the Ohio State College of Arts and Sciences Honors Research Scholarship and International Research Grant, as well as funding from the Friends of Orton Hall which enabled me to travel to Iceland in the summer of 2012 to do field research.

My research group has been incredibly supportive and helpful over the three years in which I worked on this project. Jameson, aka "Dino", helped introduce me to the software programs which were used to generate the diagrams for this paper and he accompanied me on my journey to Iceland. Fellow undergraduate researchers Chrissy and Shannon assisted me by asking questions about their research which helped further my abilities as a presenter and increased my own understanding of my work. Mention of my research group would not be complete without the inclusion of my advisor, Dr. Michael Barton. His introductory petrology course got me interested in working on volcanoes and through three years as his pupil, I have learned a number of valuable things such as how to format and write grant proposals, abstracts, and statements of purpose. He has shown me how to create a poster

for presentation at professional conferences and he has driven me to pursue questions beyond that of a typical undergraduate research project.

Finally I would like to thank the three gentlemen who made my undergraduate experience in Ohio State's Earth Science Department an enjoyable and memorable one. Nick Leeper, Jeff Thompson, Alex Rytel were the first three people I really got to know in the School of Earth Sciences. I had been a bit of a loner until field camp, but Alex convinced Jeff and Nick that I was a good person and would make a good roommate at field camp. That summer we all became close friends and they have shaped my life in a positive fashion to this day. Nick kept me grounded and showed me that I didn't need to dedicate all my time to schoolwork. Having fun has an important place in the undergraduate experience. Jeff has been a great scholarly influence on me. We always bounce ideas off each other for class, projects, his budding DJ career, among other things. He will always be a great friend and colleague. And I cannot forget Alex. Without his belief in me, I never would have been a part of this great group of friends. He has always been that emotionally stable rock I can come to for guidance in the stormy sea which is my life. His calming demeanor has inspired me to let go of stress and live a more zen lifestyle, which has improved my quality of life immensely. Thank you three for making my undergraduate experience one I will never forget, and here's to seeing you all down the road.

List of Figures

Introduction

Iceland is home to some the most active volcanoes in the world, and recent eruptions emphasize the need for additional studies with the goal of better understanding the volcanism and tectonics along this region of the Mid Atlantic Ridge. Historical patterns of eruptive activity, a growing cryptodome on the volcano's northwest flank, and an increase in earthquake frequency beneath the Myrdalsjokull ice cap suggest that Katla is showing signs of an impending eruption. The last major eruption of Katla occurred in 1918 and caused massive jökulhlaups (glacial outburst floods) which carried enough tephra and sediment to temporarily extend the southern shoreline of Iceland by 5 kilometers. The eruption also generated enough airborne tephra and ash over several weeks to cause a brief drop in global temperature (Sveinsson, 1919). A future eruption similar to the 1918 event could have serious global consequences, including severe disruptions in air travel, short-term global cooling, and shortened growing seasons.

In order to provide better estimates of the time it would take for magma to reach the surface during an eruption, the depth and structure of the magma plumbing system of a volcano must be determined. This can be done through various means such as geodetic, seismic and petrological methods. For the study of Katla, geodetics had already been done and seismic studies gave limited results due to the presence of the Myrdalsjokull ice cap above the caldera (Sturkell et al., 2003; Gudmundsson et al, 1994). Petrological methods were utilized to determine the pressure, and hence the depth, of crystallization of the magma in this study. In addition to better forecasting volcanic eruptions, determining the depth of the magma chambers beneath Katla has important implications for the study of Iceland's volcanism and tectonics as a whole. Knowing the depths of magma bodies helps constrain models for magma evolution. It also provides information about thermal gradients in the crust and how seismic velocity and density vary with depth. Finally, knowledge of the depth of

magma chambers gives insight into the crustal accretion and differentiation processes present in Iceland.

In this thesis, I am reporting the evidence for a primary magma body located in the lower crust beneath the central volcano Katla, of Iceland's Eastern Volcanic Zone (EVZ). Pressures of crystallization for the magma were determined by using an experimentally derived method developed by Yang et. al (1996) which looks at the crystallization assemblage of olivine, plagioclase and clinopyroxene along the cotectic. The results offer a different perspective than the long-standing interpretation from geophysical studies. I attempt to show how both the geophysical and petrological interpretations synergize with each other, and how the results from Katla compare and contrast with the nearby Hekla and Grímsvötn volcanoes. I use these comparisons to generate interpretations of the structure of the crust, the magma plumbing systems of the volcanoes, and mechanisms of magma evolution.

Geologic Background

The island nation of Iceland is located at the intersection of the Kolbeinsey and Reykjanes Ridge segments of the Mid-Atlantic Ridge. The crustal thickness ranges 10-40 km, which is abnormally thick for a region along a mid-ocean ridge where crustal thicknesses are normally around 5 to 8 km (Gudmundsson, 2000). Most scientists believe that the thicker crust of Iceland is due to the presence of a mantle plume which is interacting with the spreading ridge system. Current seismic studies have placed the center of the plume beneath the eastern half of Iceland where the majority of active volcanoes are located (Wolfe et al, 1997). The dating of similar volcanic rocks from both sides of the Atlantic Ocean which have been attributed to the plume indicate an initiation age of 58 to 64 million years. This coincides with the rifting event which opened the North Atlantic Ocean. Volcanic activity in the North Atlantic Igneous Province has moved eastward through time from Greenland, to Iceland's Western Volcanic Zone (WVZ) which includes the Reykjanes Peninsula, to the current

zone of activity, the EVZ, which includes many of Iceland's most active volcanoes such as Katla, Grímsvötn, and Eyjafjallajökull. The eastward movement of the plume slowly decreased the frequency of volcanism in the WVZ and has caused it to become relatively inactive as the focal point

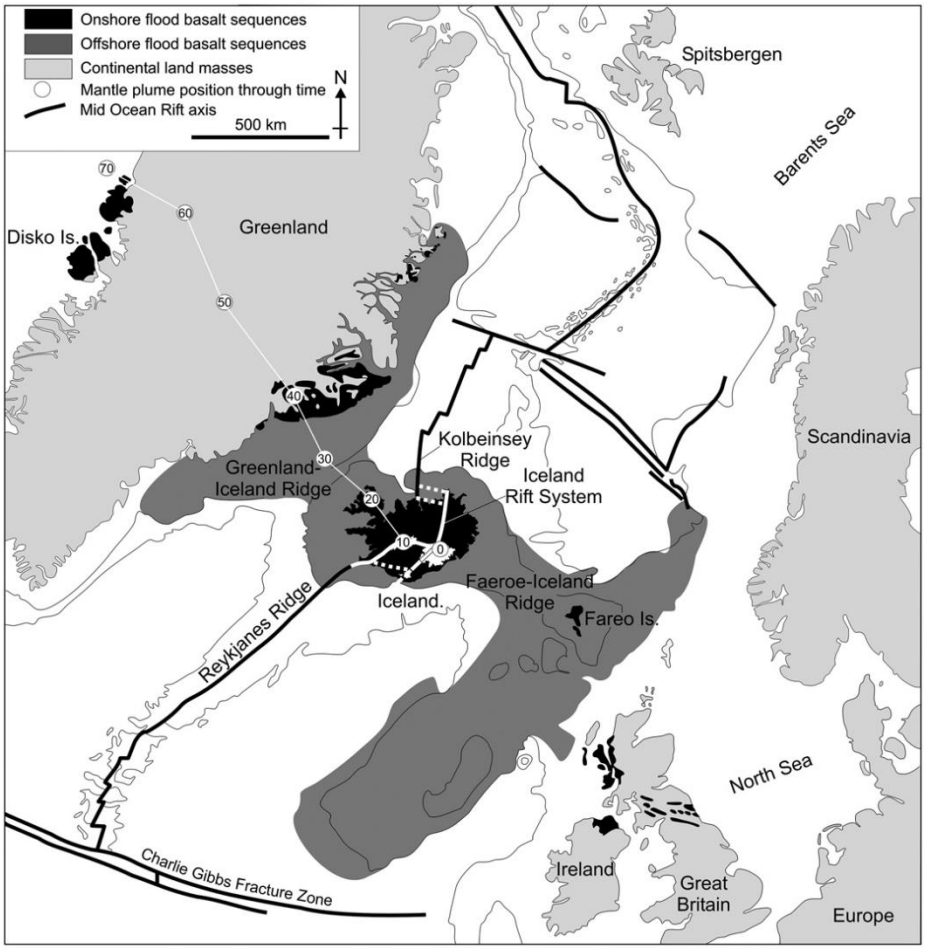

Figure 1: Iceland is a basalt plateau situated at the junction between the Reykjanes and Kolbeinsey Ridge segments of the Mid-Atlantic Ridge. From Thordarson and Larsen, 2007.

for volcanism has shifted to the EVZ (Jakobsson, 1979).

The Mid-Atlantic Ridge does not take the form of a simple linear spreading zone as it bisects Iceland. Several segments and transforms make up the complex tectonic structure of Iceland and divide it into distinct loci of spreading. The Reykjanes Volcanic Belt (RVB), Western Volcanic Zone (WVZ), Mid-Iceland Belt (MIB), and North Volcanic Zone (NVZ) are connected to the Mid-

Atlantic Ridge by the Tjörnes Fracture Zone in the north of Iceland, and by the Reykjanes Ridge in the southwest (Gudmundsson, 2000). The southern portion of the EVZ is propagating toward the southwest and scientists speculate that this segment will ultimately intersect the Reykjanes Ridge when it will become the main focal point for spreading and volcanism over the next few million years. While the rate of plate motion varies from 0.77 cm/yr on westward propagating limbs to 0.82 cm/yr on eastward propagating limbs throughout Iceland's rift and transform boundaries (Johnson et al, 1972), the spreading rates for Iceland as a whole average 1.8 cm/yr. This rate is slightly below the average value for the northern Atlantic of 2.5 cm/yr (DeMets, Gordon and Argus, 2010). It is widely accepted that one of the driving forces behind Iceland's volcanic activity is the presence of a mantle plume beneath the country (White et al., 1997). Recent models of the Iceland Plume show it to be a cylindrical body of hot magma which is elliptical in map view and narrows as it stretches toward to surface from the mantle. Recent seismic studies indicate a diameter for the plume of around 200 km (Allen et al, 1999) and it has a temperature of around 1,500 degrees Centigrade, which is 200 degrees hotter than the surrounding mantle (White et al., 1995). This plume provides most of the material feeding volcanic eruptions from deep and shallow crustal chambers. Models of Iceland's crust indicate a thickness which varies from approximately 10 km where the Reykjanes Ridge comes ashore, up to 40 km beneath the central highlands (Staples et al, 1997). Estimates of crustal thickness in Iceland are constantly being modified as more seismic studies are performed, and it is through correlation of my petrologic study with seismic and geodetic studies that we can constrain what I believe to be reliable magma chamber depths.

Iceland: Eruption Styles and Products

The volcanic systems in Iceland offer a diverse range of eruption styles and volcanic features. The

Figure 2: The canyon associated with 934 A.D. Eldgjá eruption measures 270 meters deep and over 600 meters wide. (Photo taken by Andrew Tenison)

architecture of a typical Icelandic volcanic system features a fissure swarm, a central volcano, or both (Jakobsson et al., 1978). Fissure swarms (also known as dike swarms) generally run parallel to the axis of the volcanic zone. They have been responsible for some of the largest eruptions of ash and magma in Iceland's history. The Eldgjá eruption in 934 AD was the largest in historic time and produced about 19 km^3 of basalt (Thordarson et al, 2001). The explosive power of the 934 eruption ripped open the earth and produced the largest volcanic canyon in the world, measuring 270 m deep and 600 m wide at its greatest. The Eldgjá fissure swarm is associated with the Katla volcanic system and many of the samples which were compiled for this study are from Eldgjá. Another famous

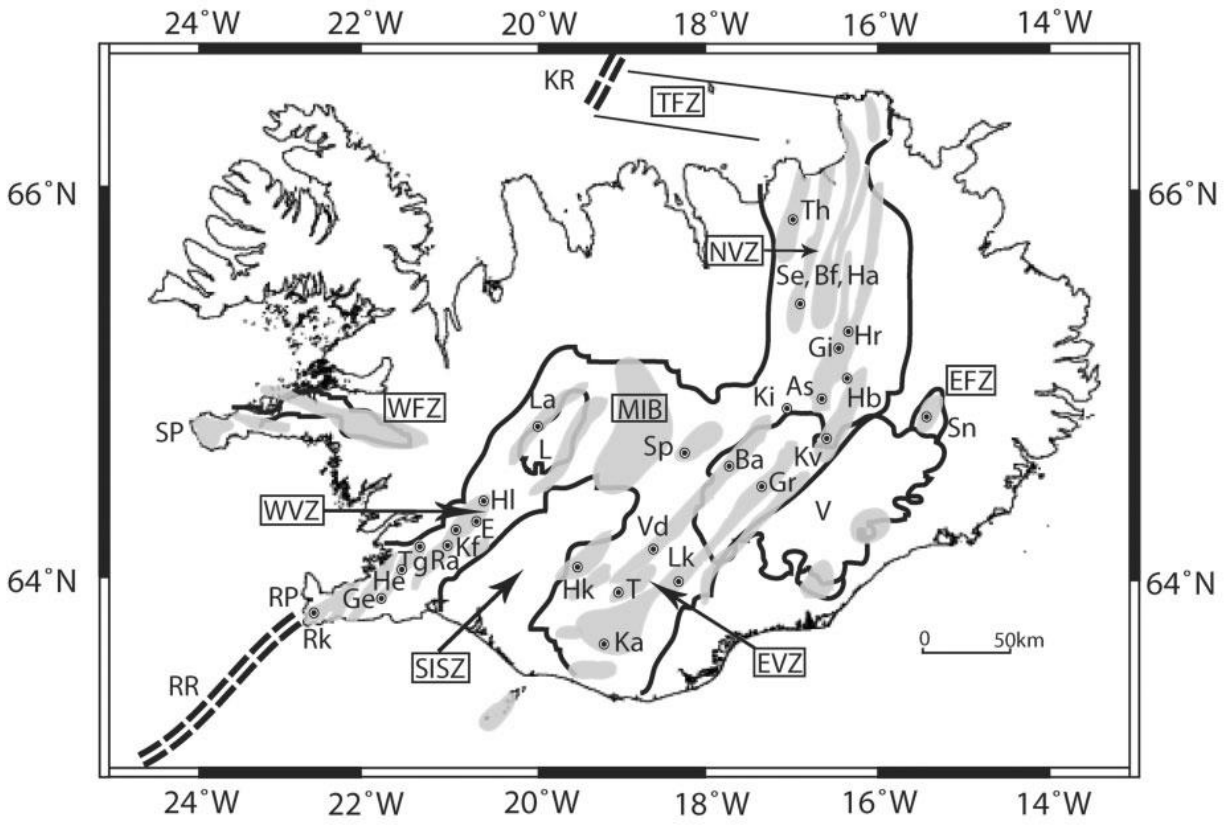

Figure 3: Location of Iceland's main volcanic centers (circles) which are discussed in this study and their associated fissure swarms (shaded region). Katla (Ka), Hekla (Hk), Torfajökull (T), Grímsvötn (Gr), Bárdarbunga (Ba). From Kelley and Barton, 2008.

fissure swarm is Laki, which is associated with the Grímsvötn central volcano. The most recent eruption of Laki took place in 1783-1784 and produced 14.7 km^3 of basalt (Thordarson and Self, 1993). The effects of this eruption were well documented globally. 120,000,000 tons of sulfur dioxide was introduced to the atmosphere over the span of the eruption. This formed a cloud of toxic gas which spread across Europe and led to the deaths of tens of thousands of Europeans. The summer months were abnormally hot in the northern hemisphere and the winters were much harsher than usual. In North America, the winter was so cold that the Mississippi River froze down to New Orleans (Oman et al., 2006). Icelandic fissure eruptions are typically characterized by a violent Strombolian eruption phase which gives way to a more effusive Hawaiian eruption style

(Thordarson and Self, 1993). Central volcanoes in Iceland tend to offer more variable eruption styles and products.

There are thirty volcanic systems in Iceland which feature twenty-three central volcanoes (Johannesson and Saemundsson, 2009). They range in form from shallowly sloped shield volcanoes, to wide caldera complexes, to stratovolcanoes. Many of the calderas are capped by a thick layer of ice, which leads to sub-glacial eruptions and jökulhlaups (flooding from glacial outbursts). Stratovolcanoes are the least common of the three primary classifications in Iceland. They are characterized by steep slopes of 15-33 degrees (Pike and Clow, 1981) and tend to produce more intermediate and silicic magma than do shield volcanoes and caldera complexes (the Torfajökull volcano being an interesting exception to this). While it would be useful to look at each volcanic system in Iceland to get the entire picture of Icelandic volcanism, it is better to take a detailed look at Katla and a few other EVZ volcanic systems. Katla, Grímsvötn, Hekla, Bárdarbunga and Torfajökull are some of the most active volcanoes in historical times and offer plentiful data due to their high eruption frequency.

Hekla

Hekla is the westernmost of the EVZ volcanoes mentioned above. It has erupted 23 times since the first eruption was recorded in 1104 A.D., which makes it the second most active volcanic system in

Figure 4: The top photo shows the extent of lava flows on the northwest flank of Hekla. The bottom photo shows the summit of the ridge shaped stratovolcano. (Photo taken by Andrew Tenison)

the Eastern Volcanic Zone (Thordarson and Larsen, 2007). Hekla is a stratovolcano but it does not take the usual conical form of most other stratovolcanoes. It forms a ridge due to the presence of fissures which run southwest to northeast, and at the central vent, the volcano rises to a height of 1,500 meters (Kjartansson and Gronvold, 1983). Vast fields of lava cover the northwest and southeast sides of the volcano with some flows reaching upwards of 50 feet in thickness. The majority of this erupted material at Hekla is dacite to basaltic andesite in composition, which differs from the tholeiitic basalts which are common throughout Iceland and the northeast portion of the EVZ. The amount of time between eruptions appears to determine the amount of silica in the magma which is consistent with fractional crystallization and interaction with the crust. Longer periods of inactivity produce more silicic magmas. During a typical eruption at the central vent, a Plinian or sub-Plinian eruption column is produced which is later followed by a longer-lasting effusive phase (Thordarson and Larsen, 2007). Fissure eruptions also occur but they are of a much more mafic composition than the eruptions from the center (Moune et al, 2006). In historic time, the total volume of erupted material from Hekla, including both lava from fissure and central volcano eruptions, and dense rock equivalent of tephra is about 13-14 km^3 (Thordarson and Larsen, 2007).

Bárdarbunga-Veidivotn

Bárdarbunga is located at the far north portion of the EVZ near its intersection with the Mid Iceland Belt (a possible transform fault region) (Oskarsson, 1984; Saemundsson, 1979). The volcano is located beneath the massive Vatnajökull glacier (the largest glacier in Europe) and forms the second highest mountain in Iceland as it reaches a height of over 2,000 meters above sea level. Like Hekla, Bárdarbunga is a combination of fissure swarms and a central volcano. The fissures run for 190 km northeast and southwest of the 10 km wide caldera, and 60 km of the fissure are located beneath Vatnajökull (Saemundsson, 1979; Thordarson and Larsen, 2007). The Bárdarbunga-

Veidivotn volcanic system is tied with Hekla as the second most active Icelandic volcano in historic time. It is characterized by sub-glacial eruptions along fissures, and from the central volcano itself. These have produced devastating jökulhlaups in the past, and have this potential in the future as well. While Bárdarbunga has not erupted since the 1800's, it has generated a lot of earthquake activity which has been associated with the eruptions of nearby Grímsvötn. The fissure swarms of both volcanoes are thought to interact, as evidenced by the 1996 eruption along the Gjálp fissure between the two calderas (Pagli et al, 2007), and Bárdarbunga's fissure swarm even extends southwest into the Torfajökull caldera. The extension into Torfajökull, a rhyolitic volcano, shows that along the fissure system magma composition can vary drastically and some complex interactions must be occurring between magmas of different composition.

The majority of Bárdarbunga's eruptions are sub-glacial, and emit moderate amounts of tephra and lava (Thordarson et al., 2007). The fact that most eruptions are sub-glacial has contributed to the difficulty of sampling lava from this volcano to use in petrologic studies. There have also been few recent eruptions of Bárdarbunga (the most recent occurring in 1862-1864 along a fissure) which has made acquiring samples uncontaminated by interaction with water difficult. Couple the issues of physically collecting samples with the issues caused by the ice sheet in terms of acquiring accurate seismic and geodetic data, and the estimate of the depth and structure of the magma chambers beneath Bárdarbunga is questionable at best. However, from the limited data that are available, shallow and deep chambers may be present beneath Bárdarbunga, with evidence for intermediate crystallization which may occur as magma approaches the surface from depth. There also may be a series of intermediate sills and feeder dikes where magma can pool (Kelley and Barton, 2008).

Grímsvötn

The Grímsvötn volcanic system is located about 20 km southeast of Bárdarbunga near the

Figure 5: The photo on the left shows one of Laki's typical cinder cone rows which run along fissures parallel to the spreading zone of the EVZ. The photo on the right is looking northeast from Laki toward the Vatnajokull ice sheet and Grímsvötn. (Photos taken by Andrew Tenison)

northernmost extent of the EVZ. Like Bárdarbunga, Grímsvötn is also located beneath the massive Vatnajökull glacier. The central caldera of the Grímsvötn system is about 8 km wide, and fissure swarms extend for 90 km NE to SW around the volcanic center. These fissures trend northeast to southwest, with 60 km located beneath ice, and the other 27 or so km are exposed as part of the Laki fissure system which was discussed earlier. The fissure swarms are marked by rows of tightly packed cones which follow a roughly linear trend across the landscape (Thordarson and Self, 1993). Grímsvötn has erupted about 70 times in recorded history, which makes it the most active of Iceland's volcanic systems (Thordarson and Larsen, 2007). Over the past 30 years, Grímsvötn has erupted four times with the most recent eruption occurring in 2011. The 2011 eruption was not a fissure eruption. It was centered at the caldera and began on May 21, 2011, when the sub-Plinian eruption column broke through the ice and rose to a height of 20 km (Gudmundsson, 2012). The eruption lasted for a mere seven days but was still the largest Iceland had seen since the late 1800's.

The ash cloud generated by the eruption caused major delays of air travel in Europe and was famously responsible for delaying President Barack Obama's European visit.

Like Bárdarbunga, Grímsvötn is characterized by fissure and sub-glacial eruptions. Lava and tephra collected from Grímsvötn and associated fissures indicate a tholeiitic basalt composition which is quite similar to Bárdarbunga. Seismic and geodetic studies have been interpreted to indicate a shallow magma chamber at 3-4 km depth (Alfaro et al, 2007). Petrologic studies (Kelley and Barton, 2008) show the presence of a magma chamber at 12-15 km depth. It is possible, given the proximity to Bárdarbunga, that the two volcanoes may have chambers which interact with each other but at this stage that hypothesis is purely speculative.

Torfajökull

Most of the following information about Torfajökull was taken from Saemundsson (2009). When compared to the other volcanoes of the EVZ (with the exception of Hekla), Torfajökull seems quite unusual. Despite not being one of the most active volcanoes in the Eastern Volcanic Zone (it last erupted in 1477), the unusual compositional variation of magma at Torfajökull, and its structure warrant further discussion within the context of the EVZ. Torfajökull is located southeast of Hekla and to the southwest of Bárdarbunga and Grímsvötn. The central volcano is characterized by very shallow sloping flanks which lead up to a 12 by 18 km wide caldera. This is odd for a volcano which primarily erupted rhyolitic and intermediate magma. Generally, volcanoes which produce rhyolites form steep-sided stratovolcanoes. Another unusual feature of Torfajökull is the composition of its magma. When it developed, Torfajökull erupted intermediate magma between alkali and tholeiitic composition. As spreading of the EVZ continued, caldera collapse occurred and Torfajökull began to produce transitional rhyolitic lavas. Subglacial rhyolitic lava domes began to erupt after the caldera collapsed around 80,000 years ago. Around the same time, basaltic material was being erupted form a southwest to northeast running dike swarm outside the caldera boundary (Saemundsson, 2009).

Seismic and geodetic studies have been conducted at Torfajökull and found a magma chamber to exist at a depth between 8 and 14 km (Soosalu and Einarsson, 2004). In recent times, eruptions have primarily been centered along the dike swarms and have been a mix of rhyolitic and tholeiitic components. The recent basalts are believed to have been triggered by injection of material from fissure swarms connecting to Bárdarbunga to the northeast. Over its lifetime, Torfajökull has produced more rhyolitic lava than all other volcanoes in Iceland combined. The fact that this sort of magma composition is present in an active rift zone where magmas supposedly trend from tholeiitic basalt to transitional alkali basalt as you go northeast to southwest along the EVZ brings into question the validity of that accepted trend in compositional variation. It does not appear that there is conclusive evidence to say that magma composition is a product of location along the Eastern Volcanic Zone, but that hypothesis still needs to be tested in a more rigorous fashion.

Katla

The final volcanic center to be discussed in the context of the EVZ rift system is also the primary focus of this study. Katla is located south of Hekla, approximately 30 km north of the southern coast of Iceland. Like Grímsvötn and Bárdarbunga, a large ice sheet called Myrdalsjökull covers the volcanic center. Katla's caldera measures around 30 km in diameter and is up to 600 meters deep (Gudmundsson et al, 1994). Katla is known to erupt from fissure swarms and from the central volcano. The most famous of the fissure eruptions was the eruptions of Eldgjá in 934 A.D. Magmas produced by Katla are of an evolved composition rich in iron and titanium (Jakobsson, 1979) but Holocene tephra layers show a cyclical eruptive pattern of mafic magma punctuated by short pulses of silicic magma (Oladottir et al, 2008). The reason for this cyclical behavior will be explained later. In terms of eruption frequency, Katla is Iceland's third most active system with at least 21 eruptions since the 9th century (Larsen 2000). The most recent large eruption occurred in 1918 and lasted 24 days. Jökulhlaup deposits containing tephra and other debris extended the southern shore of Iceland

Figure 6: The top photo is a panorama showing the Myrdalsjokull ice sheet which covers Katla. The bottom photo zooms in on the northeast flank of Katla. (Photo taken by Andrew Tenison)

seaward by 5 km. The typical amount of time between eruptions of Katla is between 13 and 95 years (Thordarson and Larsen, 2007), and the current interval is 94 years. As if this was not enough reason to monitor Iceland's sleeping giant, the 2010 eruption of Eyjafjallajökull just west of Katla was a

further cause for concern. Historically speaking, an eruption of Eyjafjallajökull tends to precede an eruption of Katla by a couple of years or so (Oladottir et al, 2008). There has been much earthquake activity at Katla's caldera from the year 2000 until the present, specifically beneath the northwest flank, but no eruption has yet occurred. In 2011 there was a small glacial outburst flood which took out some roadway along the coast, but this is not believed to have been a significant event. Similar, small-scale jökulhlaups occurred in 1955 and 1999 (Larsen, 2000).

So what do we know about Katla today that can help with forecasting when and where an eruption may take place? Seismic data collected over the past two decades show that the majority of earthquake activity at Katla occurred beneath the northwest flank of the volcano outside the caldera boundary. The earthquakes are generated at a very shallow depth of about 1.5 km and form a lens shape, which seismologists interpret as the intrusion of hot, viscous magma into a cryptodome (Soosalu et al., 2006). There are few examples of cryptodome eruptions in Iceland, but a similar famous event in North America it can be compared to is the eruption of Mt. St. Helens. Prior to this study, seismologists attempted to penetrate the thick Myrdalsjökull ice sheet with seismic undershooting to detect the possibility of a shallow magma chamber beneath the caldera. Forty seismic stations were set up along a northwest to southeast profile across the caldera and explosions were created to generate seismic waves. The results from this study by Gudmundsson et al. (1994) found that a "strong velocity depression" was present at a depth of 2 to 3 kilometers beneath the center of the Myrdalsjökull glacier. The presence of a shallow chamber such as this is not unusual for EVZ volcanoes, but the lack of a deeper magma body was troubling. Seismic waves have difficulty penetrating ice, and that only makes good resolution at greater depths even more unlikely. With a lack of reliable deep seismic data, I turned to analysis of the magma through petrology as a way to determine whether a deep magma body existed beneath Katla. I also sought to determine the

structure of the magma chamber, the means for magma differentiation, and the possible insights this may provide for crustal thickness and density of the Eastern Volcanic Zone.

Methods

The data used for analysis can be found in four papers which were published in scientific journals. The first dataset we used was published by Lacasse et al. in 2006. For that study, two field expeditions to the Myrdalsjökull ice cap and the glaciated southeast region of the volcano were conducted; one in 1995 and one in 2002. They sampled basaltic lava flows from Eldgjá, rhyolitic lava sequences, and tephra and jökulhlaup deposits. The data used from Lacasse's study were the Eldgjá samples because I was only interested in the mafic components. X-ray fluorescence (XRF) and inductively coupled plasma mass spectrometry (ICPMS) were used to analyze the whole rock samples, and electron microprobe analysis was used on the volcanic glass from tephra and pyroclastics. The chemistry of the lavas is reported in weight percent oxides (Lacasse et al., 2006). The second dataset was published by Thordarson et al. in 2003. Thordarson et al. were looking at sulfur degassing during the 934 A.D. Eldgjá eruption and collected samples of air-fall tephra, lava and vent deposits. An electron microprobe was used to determine the glass inclusion and groundmass glass composition of the samples reported as weight percent oxides (Thordarson, 2003). The third dataset of compositional data from was from Meyer et al. and was published in 1985. Meyer et al examined a wide range of Icelandic lavas, and the data used for Katla were taken from hyaloclastite tuffs and pillow basalts. As with the previous two studies, an electron microprobe was used to determine the groundmass glass composition of the lava (Meyer et al., 1985). The final dataset was published by Óladóttir et al. in 2008. The goal of her research was to analyze Katla's eruption history and magma chamber evolution by looking at a stratigraphic sequence of tephra layers from east of Katla. The glass compositions were determined as weight percent oxides by electron microprobe analysis (Oladottir et al, 2008). The total amount of data points taken from all

four publications numbered 142 samples. After data filtration (described below), this number dropped to 117 samples.

The purpose of collecting the glass samples is to determine the pressure of crystallization of the magma, which can be done by comparing the glass composition to the compositions of liquids lying along the pressure-dependent cotectic for the primary constituents of basalt: olivine, plagioclase and clinopyroxene cotectic. Several models have been proposed to describe the compositions of liquids lying along the cotectic, and I chose that devised by Yang et al. (1996) for mid-ocean ridge basalts. Yang et al conducted 190 experiments on basalt compositions over a pressure range of 0.001 to 10 kbar. The sequence for mineral crystallization in the experimental samples was olivine, plagioclase and then clinopyroxene. Empirical expressions were formulated to explain the compositional and temperature variations within the basalts over a range of pressure (Yang, Kinzler and Grove, 1996) and it is these expressions that were used in my calculations. In order to calculate depth from the pressures of crystallization, I used a conversion which took pressure over product of crustal density and the gravitational constant. The value of 2,900 kg/m^3 is the crustal density for mid-ocean ridge basalt which is the primary composition of Icelandic magmas.

Most of the data processing was done using the Microsoft Excel program described by Kelley and Barton (2008). The four compositional data sets were imported and processed to the crystallization pressure and temperature for each calculated pressure. Uncertainty values given as one standard deviation were produced for each sample. 1σ values for pressure were used as part of the data filtration process, with samples having 1σ values greater than 1.26 being removed. The 1.26 value marks the point where the level of uncertainty falls outside the acceptable range for data formed experimentally at known pressures. Another mode of filtering involved looking at the ratio of CaO/Al_2O_3. Any sample which had a value above 0.85 was discarded, as such high ratios are likely to reflect magma-crust interaction as according to conversations with Dr. Barton in 2012. Samples

were also removed if they had silica weight percent above 52%. With that high silica content, magma cannot be classified as basaltic and data from those samples cannot be considered reliable for a method which was developed for mid-ocean ridge basalts. After this filtering was complete, the data were imported into the Cohort statistical analysis and plotting program. Various combinations of the minerals olivine, plagioclase, and pyroxene are expected to crystallize out of the natural melts and these produce characteristic chemical variations in liquid compositions that are displayed on plots versus MgO. The main plots examined were for calcium, aluminum, iron, titanium, potassium, calcium-aluminum ratio, and iron-magnesium ratio. All of these components were plotted against MgO which is useful for showing olivine crystallization, which virtually always occurs in mafic magmas. Variation diagrams reveal the trends in melt (glass) composition and, from these diagrams, the mechanism of magma differentiation can be discerned and final filtration of the data occurs. If data points lie anomalously far from the main trend line in a plot, we identify and cross-analyze it with other plots to see if the composition of the sample appears to be unusual. After all the data from Katla were filtered and plotted, 117 of the original 142 samples remained. Five samples were from the Lacasse paper, 4 from Meyer, 3 from Thordarson, and 105 from the Óladóttir stratigraphic data set.

Other Methods

The Kelley/Barton method used in this study is not the only means for determining pressure of crystallization of magmas. A paper published in the Journal of Petrology by Claude Herzberg in 2004 outlines an alternate method for calculating pressure of crystallization. In order to figure out which method is best suited for use on Iceland volcanics, both methods were tested against the findings from seismic and geodetic studies at a location where reliable seismic could be acquired. This location was Hekla. The most recent geodetic analyses of Hekla show a magma body at a depth of greater than 14 kilometers which is consistent with findings from the Kelley/Barton method that

suggest an average depth of 17.5 kilometers. The results from Herzberg's method suggest an average chamber depth of around 10 kilometers. Pressures from Herzberg's method differed greatly from those obtained using the method in Yang et al. (1996) by up to 300 MPa. When the Yang et al. method was applied to analyses from a wide range of volcanic centers in Iceland, about 22% of the pressures it yielded were negative (Kelley and Barton, 2008). This is of course not a physically realistic outcome. The Herzberg (2004) method has consistently produced lower pressures than the Kelley/Barton method (11.5 km depth versus 21 kilometers for Katla) and it is because of the prevalence of negative pressures and the lack of correlation with seismic data that we use the Kelley/Barton method to determine pressures of crystallization for Katla and other Icelandic volcanoes.

Results

Pressures of crystallization for Katla were calculated and after data filtration we found that over 60% of the data points fall within a range of 6 to 7 kbar, which we take to be the location of the primary magma chamber. The scatter of data points at much lower pressure (between 1 and 5 kbar) shows

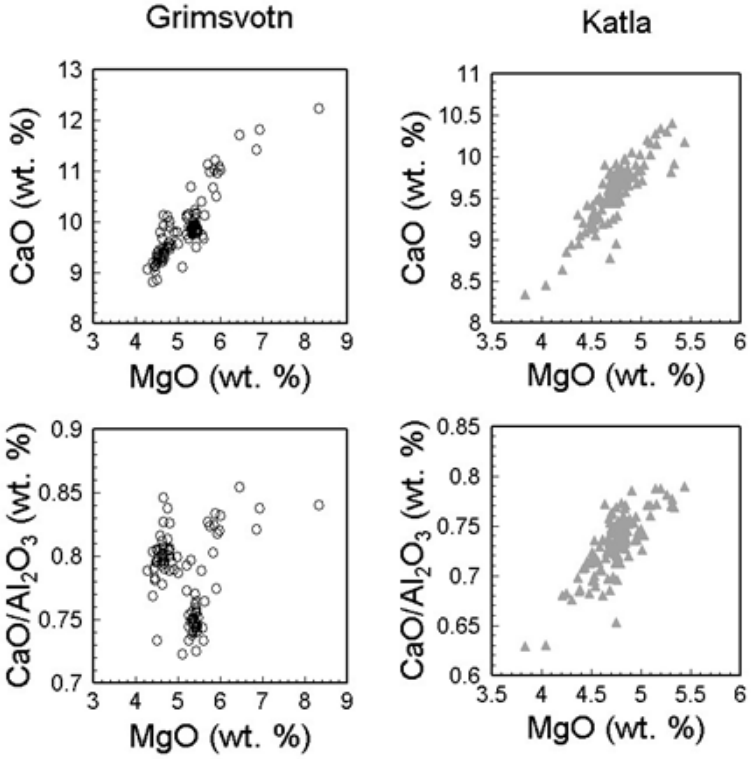

Figure 7: The above diagrams show crystallization of plagioclase and clinopyroxene in association with olivine crystallization for both Katla and Grímsvötn.

crystallization of magma on its way to the surface and higher-pressure data points show that some crystallization may occur as magma enters the chamber from the mantle. This range of pressure from 6 to 8 kbar where most of the data points lie correlates to an average depth of 22 kilometers below the surface. This agrees well with the maximum pressure (23.1 km) determined for the depth of the Katla magma chamber by Kelley and Barton (2008) using petrological methods and a smaller number of samples. A positive correlation seems to exist which relates MgO content and pressure.

This indicates crystallization as the magma approaches the surface but this this not observed at all volcanic centers (e.g. Grímsvötn) which have been studied using petrologic means. However, that may be the product of a few samples. Diagrams of CaO and CaO/Al_2O_3 ratio versus MgO also display positive relationships. These are consistent with normal crystallization of clinopyroxene and plagioclase as olivine crystallizes out of the melt. A positive relationship is also present in the diagram of FeO total versus MgO, which indicates crystallization of ferromagnesian minerals. Total iron content at Katla is generally in the range of 14-16% of the magma by weight. It is from this (as well as 4-5% TiO_2) that Katla is classified as producing Fe-Ti transitional basalts.

One of the more interesting variation diagrams which we produced was of K_2O versus time. The time axis is not commonly available for study in regards to evolution of magmas, but the tephra

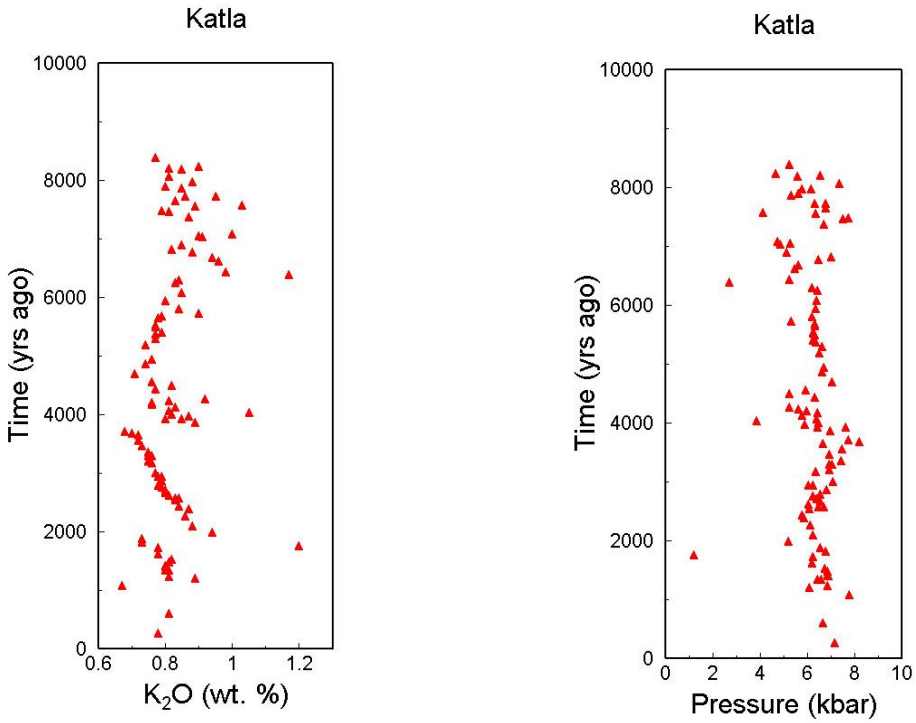

Figure 8: K_2O compositions from the Óladóttir pyroclastic data set graphed against time showing recharge and eruptive cycles. The plot of pressure versus time confirms this hypothesis as pressures would decrease during an eruptive sequence.

stratigraphic data set of Óladóttir et al. (2008) was dated using the soil accumulation rate which was based upon soil thickness after the tephra was subtracted. Carbon 14 dating of several intervals was also used to further constrain the age resolution of the samples (Oladottir et al, 2008). K_2O versus

time graphs showed a definite sequence of magma recharges and eruptions. K_2O likes to remain in the melt as magma crystallizes, so during an eruptive sequence the melt will become enriched in K_2O and during recharge from the mantle magma source, the abundance of K_2O will diminish. Several well-defined cycles are present in the K_2O versus time plot and when compared to a plot of pressure over time, there is a definite correlation. When recharge of the magma chamber is

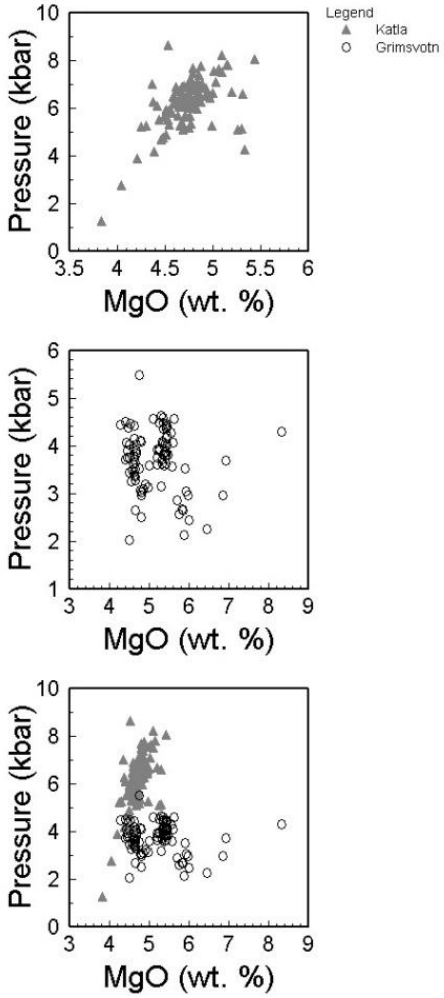

Figure 9: Location of magma chambers for Katla and Grímsvötn.

occurring, pressures are generally higher, and during an eruptive sequence pressures appear to drop as magma is crystallizing on its way toward the surface. A time axis introduces some exciting

possibilities for three dimensional plots and correlation of the trends we observe in the variation diagrams to Katla's actual recorded eruption history and this will be the next step of this work. After describing what we have seen in terms of magma variation of Katla, it is also important to mention what we did not observe. Recall that seismic undershooting of the Myrdalsjökull ice cap revealed evidence for a shallow magma body. No evidence for this appeared in the diagrams of MgO versus pressure and depth. The majority of the samples plotted in a range of 6-8 kilobars, not 1-2 kilobars. This is most likely related to the composition of the magma in this shallow chamber. In all likelihood, the magma did not show up in our data because it is of a more silicic composition than the parent transitional basalt.

Another interesting facet to look at with the Katla data is to see how it compares to other EVZ volcanoes. A deep-crustal chamber at an average depth of 22 km was located beneath Katla based upon analysis of data from our study. Previous seismic studies located a shallow chamber at 2-3 km (Gudmundsson et al, 1994). Hekla exhibits an intermediate depth chamber at 17.5 km (Kelley and Barton, 2008). Grímsvötn exhibits a slightly shallower intermediate depth chamber at around 15 kilometers, as well as a seismically determined shallow chamber at 3-4 km (Alfaro et al, 2007). Data suggest that magma bodies are common in the middle and lower crust.

Discussion

The results for pressures from Katla show crystallization of liquids along the olivine-plagioclase-clinopyroxene cotectic. Some Icelandic volcanoes exhibit variations from this cotectic such as increasing CaO with decreasing MgO, but none of those anomalies are present at Katla. When magmas ascend to the surface, they pause and crystallize for some period of time which most likely occurs in magma chambers or a system of stacked sills and dikes. When an eruption occurs, the magma quickly reaches the surface and is quenched to form glass which can be analyzed to determine the composition of the melt. The melt composition cannot be determined by looking at

phenocrysts. Depths of magma chambers are determined from pressure by taking the pressure divided by 2900 kg/m^3 as the value for crustal density time the gravitational constant. Crystallization of most chemical constituents falls along the trends which are observed for Icelandic volcanoes as a whole, but the composition in weight percent will vary from volcano to volcano. The variation diagrams reveal the possible modes of magma differentiation at Katla. Trends in CaO, MgO and Al_2O_3 are consistent with fractional crystallization as the dominant factor in compositional variance. Another mode of differentiation was revealed in the K_2O plot versus time. This showed that Katla goes through cycles of magma recharge and depletion. When a new batch of magma enters the chamber from depth, it mixes with the magma from the previous injection which has been crystallizing and enriches it with MgO which causes the amount of K_2O to drop in terms of weight percent. This mixing of the two magma compositions forms an intermediate composition. The amount of time between the injections of fresh magma may be one of the factors responsible for varying eruption products at Katla.

Despite primarily producing Fe-Ti rich basalts, rhyolitic products have been observed at Katla (Óladóttir et al., 2008). The evidence for silicic eruptions at Katla has been known for quite some time, but through a synthesis of seismic studies, stratigraphic analysis of tephra layers, and the petrologic study completed herein, a full picture of Katla's recent eruptive history begins to develop. Recall the K_2O versus time plot. When K_2O is at low levels, a fresh batch of magma has been introduced to the deep magma chamber and the system is in a period of low activity. This magma is not interacting with the magma which was left in the shallow chamber from the previous cycle of eruptive activity. The shallow magma is interacting with Iceland's gabbroic crust and crystallizing to become more felsic than the parent magma. This is why the shallow magma body did not appear in our petrologic study, but was identified at 3-4 km depth through seismic studies (Gudmundsson et al, 1994). As volcanic activity increases, this shallow chamber is forced to erupt before the more

mafic material from depth ascends. This would produce a thin layer of silicic tephra, followed by a thicker sequence of mafic tephra, which is what is observed in the study conducted by Óladóttir et al. (2008).

Crustal Thickness and Structure of Magma Plumbing System

Now that the depth of the primary magma body has been determined for Katla, it is important to figure out how it relates to the structure if Iceland's crust and see what we can infer about the structure of the magma plumbing system. Crustal thickness in Iceland is greatest over the center of the mantle plume (40-41 km) near Vatnajökull and lowest in northwest and southwest Iceland (less than 20 km). The thick crust near the plume's center is due to its active upwelling and high temperatures which enhance the production of magma. The distance to the Mohorovičić discontinuity near Katla is approximately 24 km according to combined seismic studies and gravity modeling (Darbyshire, White and Priestley, 2000). An older study by Bjarnason et al. (1993) found similar results. With Katla's deep magma chamber at 22 km below the surface, it would appear that the magma which feeds Katla ponds at the base of the crust. The reasons magma forms chambers at varying depths is not understood well but some of the influencing factors may be the buoyancy of the melt and how stress factors in the crust create zones of weakness in which magma can penetrate and accumulate (Gudmundsson, 2000). In addition to the magma chamber at Katla falling at the crust-mantle boundary, other volcanoes exhibit this. Petrologic studies of Geitafell and Hengill exhibit chamber depths of 17.8 km and 18.9 km respectively which agree well with seismic data (Bjarnason et al, 1993). This suggests crustal thicknesses of 16 km and 17.5-24 km for each volcanic center. Chamber depths for Grímsvötn (12-15 km) do not agree with their estimated respective crustal thicknesses (25 km) and are indicative of magma chambers at intermediate depths in the crust. Many EVZ volcanoes also have shallow chambers (e.g. Grímsvötn, Katla, Bárdarbunga and Eyjafjallajökull). A common factor which ties the shallow chambers together is that they are all

present beneath ice-covered calderas and they may correspond to a density boundary at the base of the upper crust (Kelley and Barton, 2008; Darbyshire, White and Priestley, 2000). Pressure data for the volcanoes of the EVZ tell us that a wide range of plumbing system structures exist in Iceland's crust. These shallow, intermediate and deep crustal chambers are likely connected by a complex series of dikes and sills. The resolution of data is over such a large range in some cases that it is impossible to determine the presence of stacked sills and dikes. At Katla for instance, the majority of the data fall within an estimated depth range of 20-26 kilometers (22 km average depth, plus or minus the standard deviation of ~3.5 km). This may indicate several interconnected sills in the lower crust or a large zone of ponding magma which crystallizes in a mush zone at the crust –mantle boundary. These diverse structures no doubt have an important effect on magma differentiation along the EVZ.

It may be that within the EVZ, there is a connection between erupted magma composition and location of a volcano along the southwest-propagating rift. Analysis of the chemistry of Katla's magma shows that it indeed has high amounts of Fe and Ti which is consistent with the consensus that Katla erupts Fe-Ti rich transitional basalt. When this composition is contrasted with other EVZ volcanoes, a wide range of compositions are observed which does not strongly support the hypothesis of magma composition varying with location along the EVZ. Bárdarbunga and Grímsvötn erupt primarily tholeiitic basalts, Torfajökull produces rhyolite and Hekla produces dacite to basaltic andesite (Thordarson and Larsen, 2007). This variation in magma composition more likely results from differences in the structure of magma plumbing systems and their location within the crust or crust-mantle boundary. The various methods of magma differentiation such as fractional crystallization, magma mixing, and assimilation also strongly affect magma composition. It seems ill-considered to attempt to label magmas of the EVZ as tholeiitic to transitional alkalic as one moves southwest along the spreading zone.

Conclusions

Pressure of crystallization for magma from Katla, as well as some other EVZ volcanoes, was calculated by a method developed by Yang et al. (1996). This method is for melts which lie along the olivine-plagioclase-clinopyroxene cotectic. After data filtration, pressures were calculated for 117 glass samples from Katla and its associated fissure eruptions. The primary range for pressure of crystallization from these samples lies between 6-8 kilobars which translates to an average depth for the magma chamber of 22 km. When this depth is compared to crustal thickness beneath Katla, the magma chamber is located near the crust-mantle boundary (Darbyshire et al., 2000). This, in addition to data from other Icelandic volcanoes, supports the hypothesis that magma ponds at the base of the crust in deep magma chambers before it ascends to the surface. In addition to this deep magma chamber, seismic studies have shown the presence of a shallow magma chamber at a depth of 3-4 kilometers below the surface (Gudmundsson et al, 1994). This chamber does not show up in petrologic data, but through correlation with the Óladóttir study (1998) of tephra stratigraphy, I am able to conclude that this shallow chamber produces viscous, silicic magma. This occurs because of fractional crystallization of the magma and crustal contamination in the shallow chamber as it is in stasis. By looking at variation diagrams of major elements along the olivine-plagioclase-clinopyroxene cotectic, I was able to identify fractionation as an important mode of magma differentiation. Plots of K_2O versus time show that magma mixing also occurs.

Throughout the Eastern Volcanic Zone in Iceland, there is a wide range of magma compositions and magma chambers occupying shallow, intermediate, and deep portions of the crust. It has been proposed by many scientists that the location of a volcano within the confines of the EVZ determines the composition of its magma. While this may be true (volcanoes closer to the Iceland plume seem to erupt more tholeiitic material because the chambers recharge and erupt more frequently than volcanoes further to the southwest), there are many more factors at play than just

location. The wide range of depths over which magmas crystallize, the quantity, depth and structure of magma plumbing systems, and the modes of magma differentiation (fractionation, assimilation, magma mixing) have an undeniable impact upon composition and further study of this very active region of the Earth's crust will only make this picture clearer.

References

Alfaro, R., Brandsdottir, B., Rowlands, D.P., White, R.S., and Gudmundsson, M.T., 2007, Structure of the Grimsvotn central volcano under the Vatnajokull icecap, Iceland: Geophysical Journal International, v. 168, p. 863-876, doi: 10.1111/j.1365-246X.2006.03238.x.

Allen, R.M., Nolet, G., Morgan, W.J., Vogfjord, K., Bergsson, B.H., Erlendsson, P., Foulger, G.R., Jakobsdottir, S., Julian, B.R., Pritchard, M.J., Ragnarsson, S., and Stefansson, R., 1999, The thin hot plume beneath Iceland: Geophysical Journal International, v. 137, p. 51-63.

Bjarnason, I.T., Menke, W., Flovenz, O.G., and Caress, D., 1993, Tomographic image of the Mid-Atlantic plate boundary in southwestern Iceland: Journal of Geophysical Research, v. 98, p. 6607-6622, doi: 10.1029/92JB02412.

Darbyshire, F.A., White, R.S., and Priestley, K.F., 2000, Structure of the crust and uppermost mantle of Iceland from a combined seismic and gravity study: Earth and Planetary Science Letters, v. 181, p. 409-428.

DeMets, C., Gordon, R.G., and Argus, D.F., 2010, Geologically current plate motions: Geophysical Journal International, v. 181, p. 1-80, doi: 10.1111/j.1365-246X.2009.04491.x.

Gudmundsson, A., 2000, Dynamics of volcanic systems in Iceland; example of tectonism and volcanism at juxtaposed hot spot and mid-ocean ridge systems: Annual Review of Earth and Planetary Sciences, v. 28, p. 107-140.

Gudmundsson, O., Brandsdottir, B., Menke, W., and Sigvaldason, G.E., 1994, The crustal magma chamber of the Katla volcano in South Iceland revealed by 2-D seismic undershooting: Geophysical Journal International, v. 119, p. 277-296.

Jakobsson, S.P., Jonsson, J., and Shido, F., 1978, Petrology of the western Reykjanes Peninsula, Iceland: Journal of Petrology, v. 19, p. 669-705.

Jakobsson, S.P., 1979, Petrology of recent basalts of the Eastern Volcanic Zone, Iceland: Acta Naturalia Islandica, Issue 26.

H. Johannesson, and K. Saemundsson. , 2009, Jardfraedikort af Islandi 1:600000, berggrunnur--Geological map of Iceland 1:600,000, bedrock geology.

Johnson, G.L., Southall, J.R., Young, P.W., and Vogt, P.R., 1972, Origin and Structure of the Iceland Plateau and Kolbeinsey Ridge: Journal of Geophysical Research, v. 77, p. 5688-5696.

Kelley, D.F., and Barton, M., 2008, Pressures of crystallization of Icelandic magmas: Journal of Petrology, v. 49, p. 465-492, doi: 10.1093/petrology/egm089.

Kjartansson, E., and Gronvold, K., 1983, Location of a magma reservoir beneath Hekla Volcano, Iceland: Nature [London], v. 301, p. 139-141.

Larsen, G., 2000, Holocene eruptions within the Katla volcanic system, South Iceland; characteristics and environmental impact: Joekull, v. 49, p. 1-28.

Meyer, P.S., Sigurdsson, H., and Schilling, J., 1985, Petrological and geochemical variations along Iceland's neovolcanic zones: Journal of Geophysical Research, v. 90, p. 10, doi: 10.1029/JB090iB12p10043.

Moune, S., Gauthier, P.J., Gislason, S.R., and Sigmarsson, O., 2006, Trace element degassing and enrichment in the eruptive plume of the 2000 eruption of Hekla Volcano, Iceland: Geochimica Et Cosmochimica Acta, v. 70, p. 461-479, doi: 10.1016/j.gca.2005.09.011.

Óladóttir, B.A., Sigmarsson, O., Larsen, G., and Thordarson, T., 2008, Katla Volcano, Iceland magma composition, dynamics and eruption frequency as recorded by Holocene tephra layers: Bulletin of Volcanology, v. 70, p. 475-493, doi: 10.1007/s00445-007-0150-5.

Oskarsson, N., 1984, Monitoring of fumarole discharge during the 1975-1982 rifting in Krafla volcanic center, North Iceland: Journal of Volcanology and Geothermal Research, v. 22, p. 97-121.

Pagli, C., Sigmundsson, F., Pedersen, R., Einarsson, P., Arnadottir, T., and Feigl, K.L., 2007, Crustal deformation associated with the 1996 Gjalp subglacial eruption, Iceland; InSAR studies in affected areas adjacent to the Vatnajokull ice cap: Earth and Planetary Science Letters, v. 259, p. 24-33, doi: 10.1016/j.epsl.2007.04.019.

Pike, R.J., and Clow, G.D., 1981, Revised classification of terrestrial volcanoes and catalog of topographic dimensions, with new results on edifice volume: U. S. Geological Survey : Open File Report 81-1038.

Saemundsson, K., 1979, Outline of the geology of Iceland: Joekull, p. 7-28.

Soosalu, H., and Einarsson, P., 2004, Seismic constraints on magma chambers at Hekla and Torfajokull Volcanoes, Iceland: Bulletin of Volcanology, v. 66, p. 276-286, doi: 10.1007/s00445-003-0310-1.

Soosalu, H., Jonsdottir, K., and Einarsson, P., 2006, Seismicity crisis at the Katla Volcano, Iceland; signs of a cryptodome? Journal of Volcanology and Geothermal Research, v. 153, p. 177-186, doi: 10.1016/j.jvolgeores.2005.10.013.

Staples, R.K., White, R.S., Brandsdottir, B., Menke, W., Maguire, P.K.H., and McBride, J.H., 1997, Faroe-Iceland Ridge experiment; 1, Crustal structure of northeastern Iceland: Journal of Geophysical Research, v. 102, p. 7849-7866, doi: 10.1029/96JB03911.

Sturkell, E., Sigmundsson, F., and Einarsson, P., 2003, Recent unrest and magma movements at Eyjafjallajokull and Katla Volcanoes, Iceland: Journal of Geophysical Research, v. 108, , doi: 10.1029/2001JB000917.

Thordarson, T., Miller, D.J., Larsen, G., Self, S., and Sigurdsson, H., 2001, New estimates of sulfur degassing and atmospheric mass-loading by the 934 AD Eldgja eruption, Iceland: Journal of Volcanology and Geothermal Research, v. 108, p. 33-54.

Thordarson, T., and Self, S., 1993, The Laki (Skaftar Fires) and Grimsvotn eruptions in 1783-1785: Bulletin of Volcanology, v. 55, p. 233-263.

Thordarson, T., and Larsen, G., 2007, Volcanism in Iceland in historical time; volcano types, eruption styles and eruptive history: Journal of Geodynamics, v. 43, p. 118-152, doi: 10.1016/j.jog.2006.09.005.

Thordarson, T., 2003, Sulphur release from Holocene flood lava eruptions in Iceland: International Union of Geodesy and Geophysics General Assembly = Union Geodesique Et Geophysique Internationale Comptes Rendus De La ...Assemblee Generale, v. 2003, Week 1, p. A.207-A.207.

White, R.S., Bown, J.W., and Smallwood, J.R., 1995, The temperature of the Iceland plume and origin of outward-propagating V-shaped ridges: Journal of the Geological Society of London, v. 152, Part 6, p. 1039-1045.

Wolfe, C.J., Bjarnason, I.T., VanDecar, J.C., and Solomon, S.C., 1997, Seismic structure of the Iceland mantle plume: Nature [London], v. 385, p. 245-247.

Yang, H.J., Kinzler, R.J., and Grove, T.L., 1996, Experiments and models of anhydrous, basaltic olivine-plagioclase-augite saturated melts from 0.001 to 10 kbar: Contributions to Mineralogy and Petrology, v. 124, p. 1-18.

Appendix A: Geologic Setting

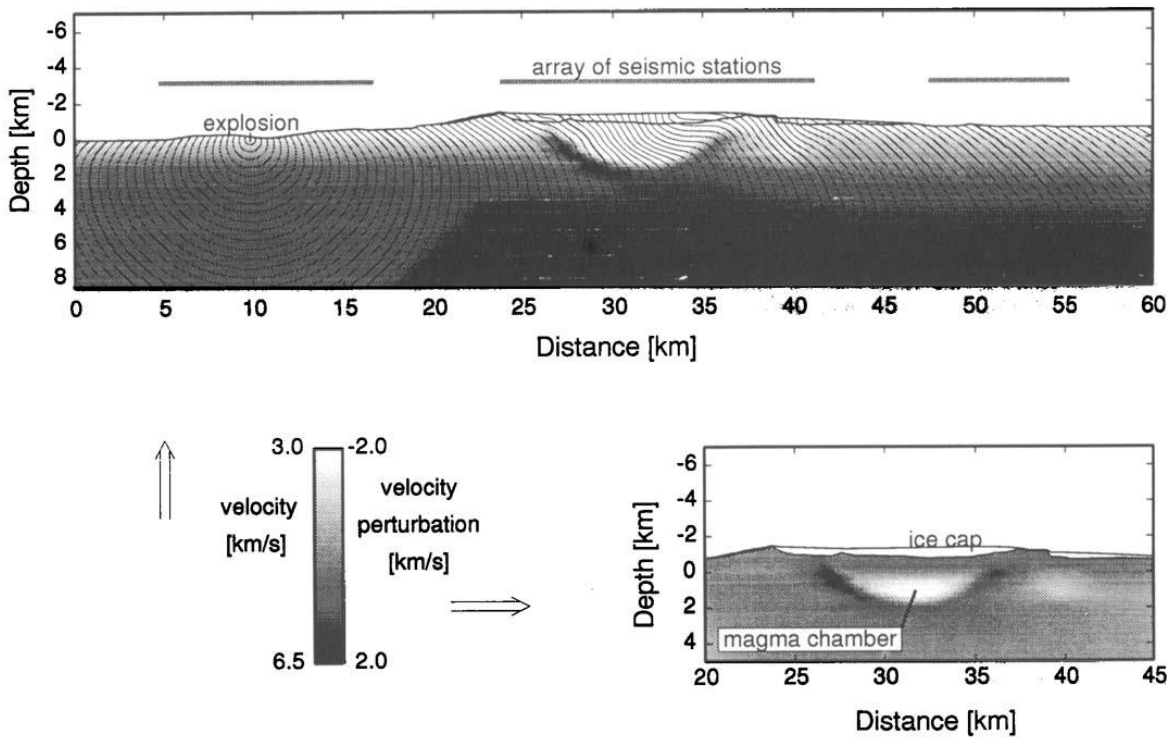

Figure A1: Seismic studies have revealed the presence of a shallow magma chamber ~3 km below Katla's ice cap (Gudmundsson et al., 1994).

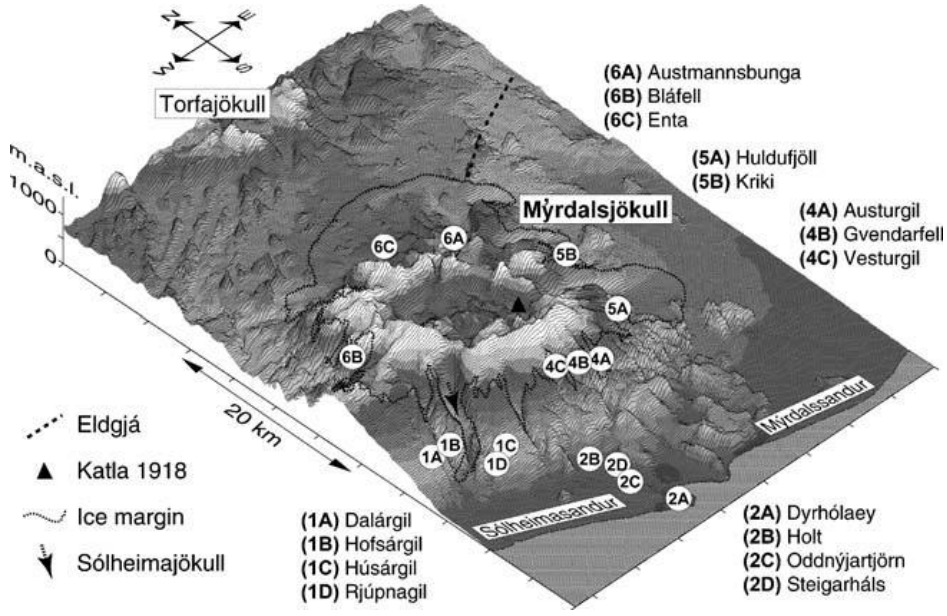

Figure A2: Diagram showing the structure of Katla's sub-ice caldera as acquired from radio echo sounding (Lacasse et al., 2006).

Appendix B: Additional Variation Diagrams

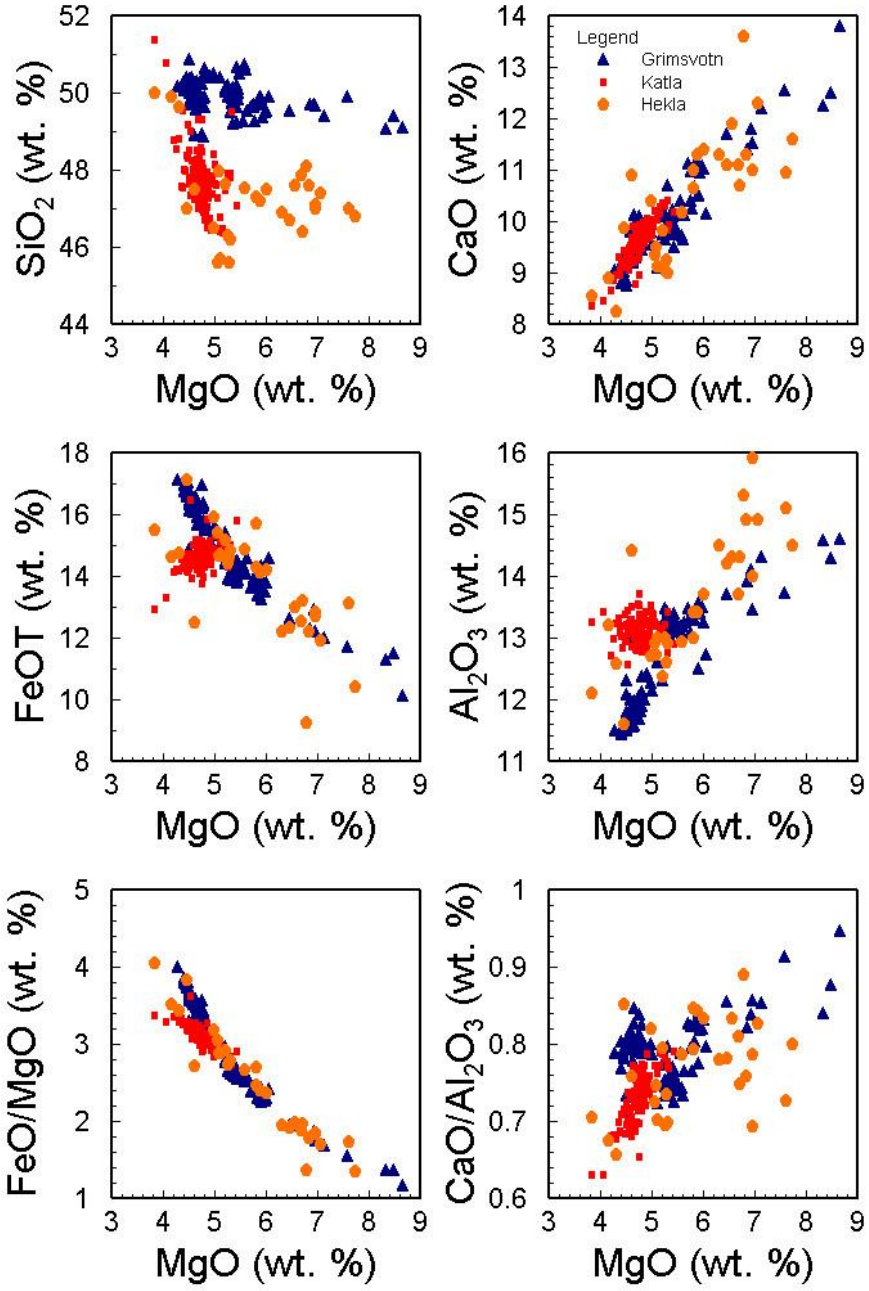

Figure B1: Geochemical trends for Grímsvötn, Katla, and Hekla showing variation in silica, iron and aluminum contents.

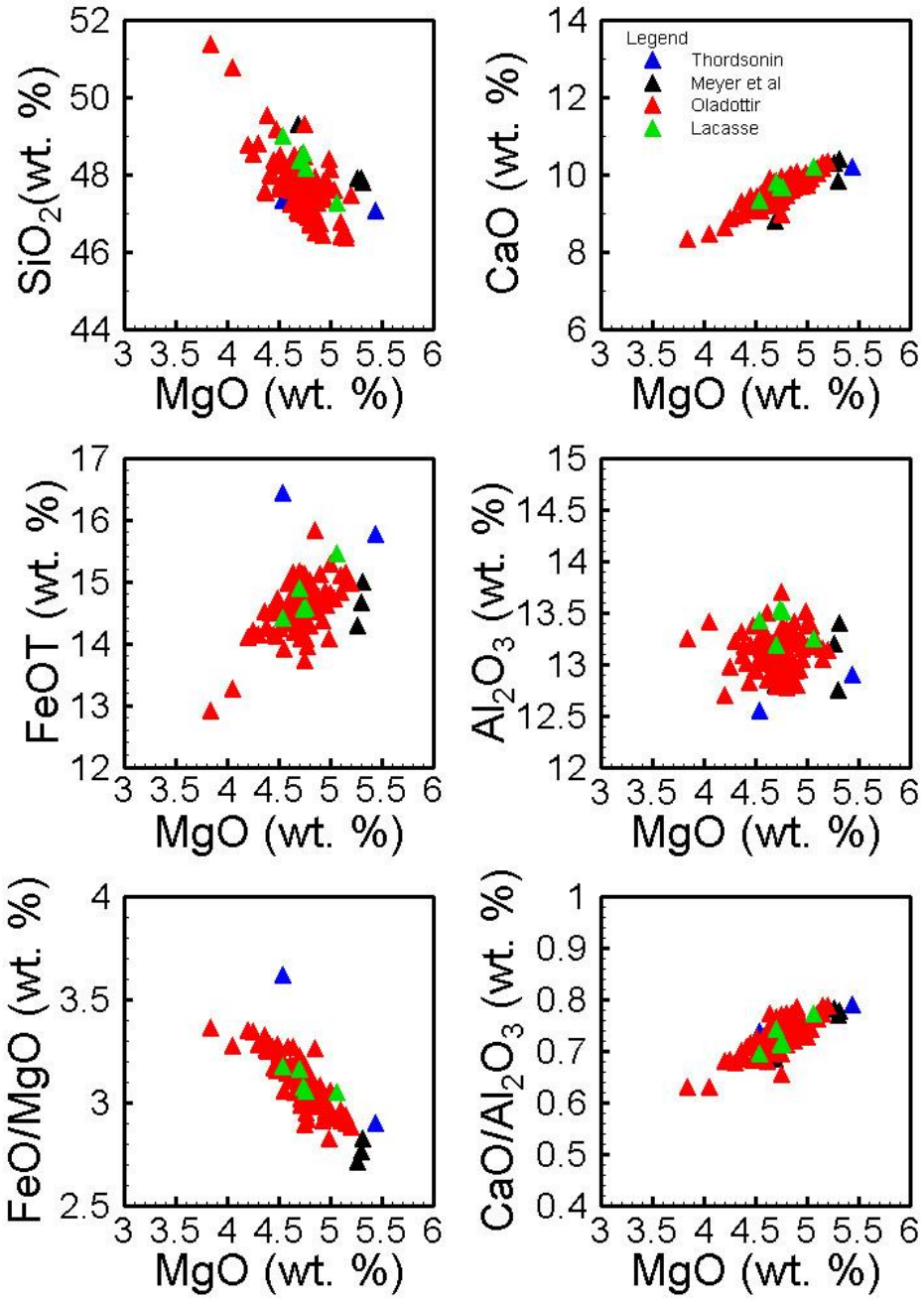

Figure B2: Geochemical trends for Katla showing crystallization of olivine, plagioclase, clinopyroxene and iron-rich minerals. Color coded based on the four data sets which were used.

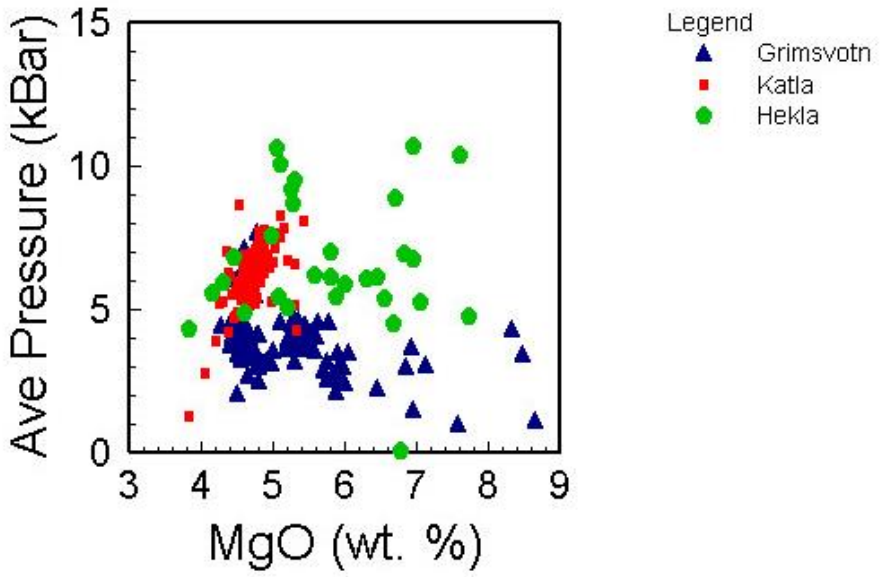

Figure B3: Combined pressure calculation for Grímsvötn, Katla, and Hekla showing Grímsvötn as having the shallowest magma chamber followed by Hekla and then Katla with the deepest.

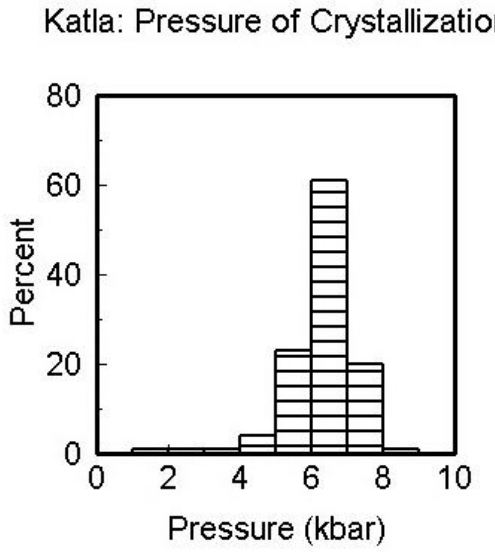

Figure B4: Histogram showing depths of crystallization of the Katla glass samples. (Bin size is 1 kbar)

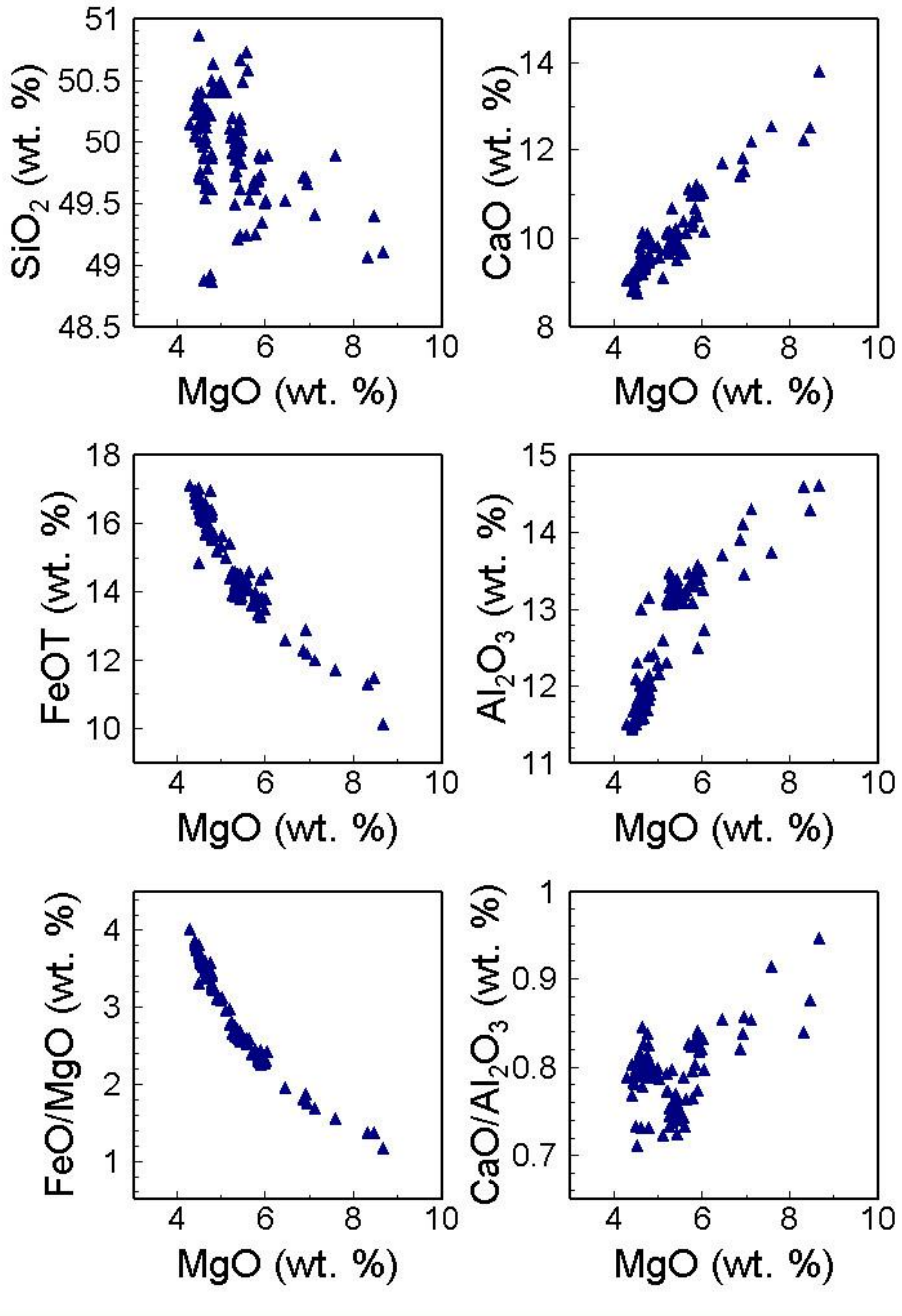

Figure B5: Geochemical variation for Grímsvötn. Unlike Katla, iron is not falling out of the melt. Normal ol-plag-cpx crystallization is present. Grímsvötn shows higher silica values than Katla.

Appendix C: Geochemical Data Tables For All Published Datasets

Location	reference	sample_id	SiO_2	Al_2O_3	TiO_2	Fe_2O_3	FeOT	MnO	MgO	CaO	Na_2O	K_2O	P_2O_5	TOTAL	Mg#	FeO/MgO	CaO/Al_2O_3	Na+K
Eldgja	Thordarson et al.	Gi13-2-665	47.04	12.89	4.29	0.00	15.76	0.22	5.44	10.17	2.62	0.61	0.42	99.46	0.3809	2.897	0.7890	3.230
Eldgja	Thordarson et al.	60888-5-1,	47.32	12.55	4.21	0.00	16.42	0.34	4.54	9.23	2.75	0.53	0.47	98.36	0.3302	3.617	0.7355	3.280
Eldgjá	Thordarson et al.	tromb Teph	49.50	12.90	2.98	0.00	14.57	0.23	5.34	9.91	2.75	0.44	0.32	98.94	0.3952	2.728	0.7682	3.190
Katla	Meyer et al. 198	EZ153G	49.30	12.80	4.04	0.00	14.79	0.27	4.69	8.77	3.12	0.84	0.49	99.11	0.3611	3.154	0.6852	3.960
Katla	Meyer et al. 198	EZ235G	47.80	13.40	3.50	0.00	15.00	0.23	5.32	10.40	2.89	0.74	0.42	99.70	0.3873	2.820	0.7761	3.630
Katla	Meyer et al. 198	EZ238G	47.89	12.75	4.26	0.00	14.66	0.20	5.31	9.81	3.22	0.64	0.35	99.09	0.3923	2.761	0.7694	3.860
Katla	Meyer et al. 198	EZ241G	47.90	13.20	4.40	0.00	14.29	0.22	5.27	10.30	3.05	0.68	0.39	99.70	0.3966	2.712	0.7803	3.730
K-1755	250	(I)	47.81	13.15	4.63	0.00	14.88	0.23	4.78	9.46	2.98	0.78	0.63	99.33	0.3641	3.113	0.7194	3.760
K-1416	589	(I)	47.57	12.84	4.75	0.00	14.63	0.24	4.62	9.44	3.09	0.81	0.76	98.75	0.3602	3.167	0.7352	3.900
Eldgjá	1070	(I)	46.34	13.05	4.40	0.00	15.13	0.22	5.15	10.27	2.91	0.67	0.46	98.60	0.3776	2.938	0.7870	3.580
AT-4	1190	(II)	48.00	13.01	4.41	0.00	14.49	0.24	4.42	9.20	3.19	0.89	0.70	98.55	0.3522	3.278	0.7071	4.080
AT-5	1230	(II)	47.22	13.13	4.62	0.00	14.71	0.24	4.62	9.67	3.23	0.81	0.61	98.86	0.3589	3.184	0.7365	4.040
AT-8-1	1325	(II)	46.98	12.84	4.58	0.00	14.67	0.23	4.69	9.67	3.11	0.80	0.60	98.17	0.3630	3.128	0.7531	3.910
AT-8-3	1325	(II)	47.36	12.98	4.60	0.00	14.72	0.23	4.68	9.50	3.11	0.81	0.59	98.58	0.3617	3.145	0.7319	3.920
AT-10	1400	(II)	47.19	12.80	4.57	0.00	15.11	0.23	4.73	9.58	3.08	0.80	0.59	98.68	0.3582	3.195	0.7484	3.880
AT-11-2	1415	(II)	46.97	12.85	4.63	0.00	15.00	0.23	4.70	9.79	3.08	0.80	0.61	98.66	0.3584	3.191	0.7619	3.880
AT-13-1	1470	(II)	47.06	12.93	4.62	0.00	14.98	0.24	4.68	9.78	3.03	0.81	0.59	98.72	0.3577	3.201	0.7564	3.840
AT-14	1510	(II)	47.36	12.91	4.62	0.00	15.00	0.24	4.77	9.62	3.05	0.82	0.57	98.96	0.3618	3.145	0.7452	3.870
AT-15	1610	(II)	46.75	12.77	4.60	0.00	14.65	0.23	4.81	9.86	3.09	0.78	0.54	98.08	0.3692	3.046	0.7721	3.870
AT-16	1715	(II)	46.95	12.90	4.58	0.00	14.74	0.23	4.75	9.91	3.01	0.78	0.53	98.38	0.3649	3.103	0.7682	3.790
AT-17	1750	(II)	51.34	13.25	3.85	0.00	12.91	0.23	3.84	8.33	3.44	1.20	0.52	98.91	0.3465	3.362	0.6287	4.640
At-18	1810	(II)	46.42	12.95	4.55	0.00	14.36	0.23	4.93	9.75	2.95	0.73	0.52	97.39	0.3796	2.913	0.7529	3.680
AT-19	1875	(II)	46.49	12.93	4.54	0.00	14.56	0.23	4.85	9.96	2.92	0.73	0.50	97.71	0.3726	3.002	0.7703	3.650
AT-21	1975	(III)	48.52	12.97	4.30	0.00	14.20	0.25	4.25	8.84	3.23	0.94	0.67	98.17	0.3479	3.341	0.6816	4.170
AT-23	2080	(III)	47.53	13.08	4.44	0.00	14.24	0.24	4.38	8.94	3.24	0.88	0.61	97.58	0.3541	3.251	0.6835	4.120
AT-25-2	2255	(III)	47.86	13.13	4.47	0.00	14.46	0.24	4.59	9.26	3.15	0.86	0.58	98.60	0.3614	3.150	0.7053	4.010
AT-26	2375	(III)	47.79	13.06	4.41	0.00	14.32	0.23	4.54	9.14	3.07	0.87	0.57	98.00	0.3611	3.154	0.6998	3.940
AT-27nh	2430	(III)	47.74	13.01	4.47	0.00	14.60	0.23	4.52	9.41	3.15	0.84	0.55	98.52	0.3556	3.230	0.7233	3.990
AT-31	2535	(III)	47.17	13.01	4.48	0.00	14.33	0.24	4.76	9.50	3.09	0.83	0.53	97.94	0.3719	3.011	0.7302	3.920
AT-33	2555	(III)	47.31	13.15	4.59	0.00	14.66	0.23	4.66	9.50	3.14	0.84	0.56	98.64	0.3617	3.146	0.7224	3.980
AT-34	2560	(III)	47.50	13.18	4.59	0.00	14.59	0.23	4.77	9.67	3.11	0.83	0.57	99.04	0.3682	3.059	0.7337	3.940
AT-37	2605	(III)	47.42	13.20	4.65	0.00	14.17	0.22	4.65	9.47	2.98	0.81	0.54	98.11	0.3691	3.047	0.7174	3.790
AT-40gr	2655	(III)	47.45	13.15	4.49	0.00	14.55	0.23	4.74	9.49	3.10	0.80	0.55	98.55	0.3674	3.070	0.7217	3.900
AT-42	2700	(III)	47.80	13.21	4.69	0.00	14.62	0.23	4.97	9.82	3.12	0.80	0.56	99.82	0.3773	2.942	0.7434	3.920
AT-43	2740	(III)	47.27	13.16	4.46	0.00	14.29	0.23	4.80	9.66	2.99	0.79	0.54	98.19	0.3745	2.977	0.7340	3.780
AT-44	2785	(III)	47.61	13.14	4.61	0.00	14.66	0.23	4.96	9.67	2.90	0.78	0.52	99.08	0.3762	2.956	0.7359	3.680
AT-50	2860	(III)	47.38	13.13	4.63	0.00	14.76	0.23	4.76	9.71	3.09	0.79	0.58	99.06	0.3650	3.101	0.7395	3.880
AT-53eh	2925	(III)	47.02	12.95	4.52	0.00	14.24	0.23	4.72	9.46	2.98	0.79	0.53	97.44	0.3714	3.017	0.7305	3.770
AT-53nh	2925	(III)	47.34	13.05	4.55	0.00	14.44	0.22	4.73	9.53	3.02	0.78	0.55	98.21	0.3687	3.053	0.7303	3.800
AT-56	2995	(III)	47.03	13.06	4.57	0.00	14.68	0.22	4.85	9.57	2.90	0.77	0.55	98.20	0.3706	3.027	0.7328	3.670
AT-61	3160	(III)	47.41	13.04	4.51	0.00	14.66	0.22	4.84	9.68	3.01	0.76	0.52	98.65	0.3705	3.029	0.7423	3.770
AT-63	3195	(III)	46.90	13.06	4.54	0.00	14.62	0.23	4.84	9.67	2.99	0.75	0.53	98.13	0.3711	3.021	0.7404	3.740
AT-66	3280	(III)	46.89	12.86	4.52	0.00	14.88	0.23	4.78	9.64	2.99	0.75	0.55	98.09	0.3641	3.113	0.7496	3.740
AT-67a	3290	(III)	47.09	13.01	4.50	0.00	14.80	0.23	4.75	9.55	3.00	0.76	0.56	98.25	0.3639	3.116	0.7341	3.760
AT-67b	3350	(III)	47.08	13.07	4.54	0.00	15.00	0.22	4.80	9.56	2.93	0.75	0.53	98.48	0.3632	3.125	0.7314	3.680
AT-71	3455	(III)	46.72	12.89	4.54	0.00	14.90	0.23	4.83	9.79	2.98	0.73	0.51	98.12	0.3662	3.085	0.7595	3.710
AT-72	3540	(III)	46.75	13.18	4.38	0.00	14.83	0.22	5.10	10.02	2.96	0.72	0.50	98.66	0.3800	2.908	0.7602	3.680
AT-75	3645	(III)	47.44	13.13	4.60	0.00	14.97	0.22	5.20	10.33	2.90	0.72	0.50	100.01	0.3824	2.879	0.7867	3.620
AT-76	3670	(III)	46.40	13.19	4.53	0.00	15.10	0.22	5.10	10.16	3.01	0.70	0.50	98.91	0.3758	2.961	0.7703	3.710
AT-77	3705	(III)	46.46	13.14	4.38	0.00	14.96	0.21	5.16	10.14	2.94	0.68	0.47	98.54	0.3807	2.899	0.7717	3.620
AT-79	3850	(IV)	47.55	13.31	4.16	0.00	14.52	0.24	4.37	9.29	3.28	0.89	0.69	98.30	0.3492	3.323	0.6980	4.170

AT-83	3910	(IV)	47.70	13.05	4.45	0.00	14.98	0.24	4.59	9.51	3.16	0.85	0.55	99.08	0.3533	3.264	0.7287	4.010						
AT-84	3920	(IV)	46.70	13.14	4.55	0.00	15.02	0.23	4.80	9.80	3.00	0.80	0.53	98.57	0.3629	3.129	0.7458	3.800						
AT-86	3955	(IV)	47.62	12.94	4.65	0.00	14.55	0.24	4.51	9.30	3.25	0.87	0.58	98.51	0.3559	3.226	0.7187	4.120						
AT-88	4000	(IV)	47.70	13.25	4.58	0.00	14.78	0.23	4.87	9.86	3.10	0.82	0.53	99.72	0.3700	3.035	0.7442	3.920						
AT-89	4025	(IV)	48.75	12.69	4.28	0.00	14.10	0.23	4.21	8.63	3.29	1.05	0.58	97.81	0.3474	3.349	0.6801	4.340						
AT-90	4050	(IV)	47.80	13.01	4.60	0.00	15.15	0.22	4.70	9.71	3.21	0.81	0.54	99.75	0.3561	3.223	0.7463	4.020						
AT-93	4110	(IV)	48.22	13.22	4.35	0.00	14.38	0.22	4.56	9.47	3.18	0.83	0.62	99.05	0.3611	3.154	0.7163	4.010						
AT-94	4160	(IV)	47.52	13.07	4.57	0.00	14.84	0.22	4.76	9.71	3.15	0.76	0.52	99.12	0.3638	3.118	0.7429	3.910						
AT-95	4190	(IV)	47.54	12.84	4.58	0.00	14.83	0.20	4.78	9.69	2.99	0.76	0.54	98.75	0.3649	3.103	0.7547	3.750						
AT-97	4220	(IV)	47.81	12.84	4.75	0.00	15.14	0.23	4.64	9.90	3.28	0.81	0.52	99.92	0.3533	3.263	0.7710	4.090						
AT-98	4250	(IV)	48.47	13.03	4.34	0.00	14.61	0.23	4.66	9.43	3.31	0.92	0.57	99.57	0.3625	3.135	0.7237	4.230						
HA-3	4425	(IV)	47.78	13.30	4.44	0.00	14.62	0.21	4.83	9.72	3.20	0.77	0.50	99.37	0.3706	3.027	0.7308	3.970						
HA-4	4480	(IV)	47.95	13.09	4.33	0.00	14.29	0.22	4.69	9.46	3.10	0.82	0.49	98.44	0.3691	3.047	0.7227	3.920						
HA-5	4540	(V)	47.26	12.85	4.49	0.00	14.61	0.21	4.84	9.70	3.12	0.76	0.52	98.36	0.3713	3.019	0.7549	3.880						
HA-7	4685	(V)	47.58	13.37	4.50	0.00	14.73	0.21	5.04	9.90	3.12	0.71	0.52	99.68	0.3789	2.923	0.7405	3.830						
HA-8	4850	(V)	47.63	13.17	4.43	0.00	14.81	0.21	5.00	9.83	3.10	0.74	0.51	99.43	0.3757	2.962	0.7464	3.840						
HA-10	4925	(V)	47.75	13.34	4.49	0.00	14.70	0.21	4.85	9.69	3.02	0.76	0.51	99.32	0.3703	3.031	0.7264	3.780						
HA-13	5180	(V)	47.36	13.04	4.53	0.00	14.85	0.21	4.95	9.89	2.96	0.74	0.50	99.03	0.3727	3.000	0.7584	3.700						
HA-15	5280	(V)	47.82	13.26	4.51	0.00	14.81	0.22	4.94	9.74	2.98	0.77	0.50	99.55	0.3729	2.998	0.7345	3.750						
HA-17	5370	(V)	47.64	13.27	4.51	0.00	14.64	0.22	4.85	9.79	3.15	0.77	0.50	99.34	0.3713	3.019	0.7378	3.920						
HA-18	5390	(V)	47.48	13.20	4.47	0.00	14.51	0.22	4.86	9.72	3.11	0.79	0.50	98.86	0.3739	2.986	0.7364	3.900						
HA-19	5480	(V)	47.56	13.04	4.53	0.00	14.94	0.21	4.81	9.85	3.06	0.77	0.52	99.29	0.3646	3.106	0.7554	3.830						
HA-20	5515	(V)	47.93	13.33	4.52	0.00	14.54	0.20	4.81	9.74	3.09	0.77	0.54	99.47	0.3710	3.023	0.7307	3.860						
HA-21	5645	(V)	47.54	13.08	4.53	0.00	14.76	0.22	4.82	9.77	3.08	0.78	0.53	99.11	0.3679	3.062	0.7469	3.860						
HA-23	5670	(V)	47.43	13.17	4.49	0.00	14.62	0.22	4.79	9.74	3.01	0.79	0.51	98.77	0.3687	3.052	0.7396	3.800						
HA-25	5720	(V)	48.25	13.00	4.61	0.00	14.78	0.23	4.67	9.58	3.11	0.90	0.52	99.65	0.3603	3.165	0.7369	4.010						
HA-26	5790	(V)	47.33	12.89	4.63	0.00	15.04	0.23	4.70	9.81	3.00	0.84	0.52	98.99	0.3578	3.200	0.7611	3.840						
HA-29	5935	(V)	47.02	12.99	4.53	0.00	14.80	0.23	4.84	9.97	3.08	0.80	0.51	98.77	0.3683	3.058	0.7675	3.880						
HA-31	6065	(V)	47.15	12.78	4.53	0.00	15.08	0.23	4.71	9.75	3.25	0.85	0.56	98.89	0.3576	3.202	0.7629	4.100						
HA-32	6210	(V)	46.71	12.80	4.48	0.00	15.12	0.23	4.91	10.05	3.05	0.80	0.54	98.69	0.3666	3.079	0.7852	3.850						
HA-33	6245	(V)	47.83	13.06	4.58	0.00	15.12	0.23	4.76	9.83	3.14	0.83	0.56	99.94	0.3595	3.176	0.7527	3.970						
HA-34	6285	(V)	47.24	13.00	4.16	0.00	14.62	0.23	4.88	9.77	3.21	0.84	0.54	98.49	0.3730	2.996	0.7515	4.050						
HA-35	6375	(V)	50.74	13.41	3.74	0.00	13.26	0.23	4.05	8.44	3.46	1.17	0.60	99.10	0.3525	3.274	0.6294	4.630						
HA-36	6430	(V)	48.78	13.22	4.21	0.00	14.13	0.24	4.31	8.93	3.39	0.98	0.67	98.86	0.3522	3.278	0.6755	4.370						
HA-38	6610	(V)	47.96	12.82	4.36	0.00	14.50	0.24	4.44	9.08	3.24	0.96	0.64	98.24	0.3531	3.266	0.7083	4.200						
HA-39	6665	(V)	48.27	12.93	4.25	0.00	14.71	0.24	4.49	9.21	3.39	0.94	0.63	99.06	0.3524	3.276	0.7123	4.330						
HA-41	6755	(V)	47.60	13.00	4.43	0.00	14.92	0.24	4.69	9.55	3.30	0.88	0.58	99.19	0.3591	3.181	0.7346	4.180						
HA-42	6810	(V)	46.60	12.93	4.25	0.00	14.74	0.23	4.89	9.79	3.21	0.82	0.56	98.02	0.3716	3.014	0.7572	4.030						
HA-43	6885	(V)	47.47	13.11	4.15	0.00	13.72	0.23	4.75	9.43	3.06	0.85	0.52	97.29	0.3816	2.888	0.7193	3.910						
HA-46	7020	(VII)	48.48	13.20	4.34	0.00	14.25	0.23	4.52	9.16	3.13	0.91	0.45	98.67	0.3612	3.153	0.6939	4.040						
HA-47nh	7040	(VII)	47.68	13.14	4.26	0.00	13.90	0.23	4.55	9.05	3.03	0.90	0.48	97.22	0.3685	3.055	0.6887	3.930						
HA-48	7075	(VII)	49.14	13.37	4.27	0.00	14.12	0.22	4.48	9.12	3.26	1.00	0.57	99.55	0.3613	3.152	0.6821	4.260						
RF-3	7235	(VII)	49.28	13.69	4.37	0.00	14.44	0.23	4.75	8.94	3.17	1.00	0.49	100.36	0.3696	3.040	0.6530	4.170						
RF-5	7365	(VII)	48.44	13.35	4.45	0.00	15.06	0.22	4.76	9.28	3.17	0.87	0.50	100.10	0.3604	3.164	0.6951	4.040						
RF-9	7460	(VII)	48.12	13.39	4.52	0.00	15.29	0.23	5.01	9.71	3.16	0.81	0.54	100.78	0.3687	3.052	0.7252	3.970						
RF-10	7470	(VII)	47.48	13.41	4.60	0.00	14.77	0.24	4.88	9.64	3.29	0.79	0.61	99.71	0.3707	3.027	0.7189	4.080						
RF-14	7550	(VII)	48.48	13.10	4.62	0.00	15.11	0.24	4.72	9.52	2.85	0.89	0.61	100.14	0.3577	3.201	0.7267	3.740						
RF-15	7560	(VII)	49.53	13.17	4.22	0.00	14.25	0.24	4.39	9.04	3.26	1.03	0.57	99.70	0.3545	3.246	0.6864	4.290						
RF-18	7635	(VII)	47.25	13.06	4.49	0.00	14.75	0.24	4.79	9.50	3.07	0.83	0.53	98.51	0.3666	3.079	0.7274	3.900						
RF-19	7715	(VII)	47.61	13.29	4.46	0.00	14.62	0.24	4.80	9.46	3.17	0.86	0.54	99.05	0.3692	3.046	0.7118	4.030						
RF-20	7720	(VII)	48.13	13.50	4.30	0.00	14.35	0.25	4.62	9.18	3.19	0.95	0.53	99.00	0.3646	3.106	0.6800	4.140						
RF-21	7735	(VIII)	47.27	12.96	4.74	0.00	14.51	0.25	4.79	9.50	3.08	0.82	0.74	98.66	0.3705	3.029	0.7330	3.900						
RF-25	7855	(VIII)	48.01	13.34	4.32	0.00	13.94	0.24	4.78	9.58	3.10	0.85	0.52	98.68	0.3794	2.916	0.7181	3.950						
RF-26	7890	(VIII)	47.94	13.36	4.21	0.00	14.07	0.24	4.77	9.61	3.02	0.80	0.51	98.53	0.3767	2.950	0.7193	3.820						
RF-28	7960	(VIII)	47.97	13.28	4.29	0.00	14.39	0.24	4.58	9.47	2.92	0.88	0.53	98.55	0.3620	3.142	0.7131	3.800						
RF-29	7965	(VIII)	47.93	13.28	4.34	0.00	14.52	0.24	4.61	9.36	3.22	0.88	0.54	98.92	0.3614	3.150	0.7048	4.100						
RF-35	8055	(VIII)	47.92	13.00	4.60	0.00	15.83	0.23	4.86	9.77	2.99	0.81	0.53	100.54	0.3537	3.257	0.7515	3.800						
RF-38	8175	(VIII)	48.05	13.23	4.39	0.00	14.08	0.24	4.72	9.24	3.18	0.85	0.52	98.50	0.3741	2.983	0.6984	4.030						
RF-40	8200	(VIII)	47.88	13.19	4.31	0.00	14.64	0.24	4.67	9.19	3.10	0.81	0.52	98.55	0.3625	3.135	0.6967	3.910						
RF-41	8230	(VIII)	48.36	13.18	4.42	0.00	14.13	0.24	4.46	9.41	3.20	0.90	0.52	98.82	0.3601	3.168	0.7140	4.100						
RF-43	8380	(VIII)	48.40	13.51	4.02	0.00	14.08	0.23	4.99	10.02	2.97	0.77	0.48	99.47	0.3872	2.822	0.7417	3.740						
Katla	Lacasse et al 20	IC95-92	48.34	13.18	4.70	0.00	14.88	0.20	4.71	9.78	3.08	0.76	0.49	100.12	0.3607	3.159	0.7420	3.840						
Katla	Lacasse et al 20	IC95-67	47.25	13.24	4.60	0.00	15.45	0.23	5.07	10.20	2.92	0.67	0.42	100.05	0.3691	3.047	0.7704	3.590						
Katla	Lacasse et al 20	IC95-74	48.14	13.51	4.17	0.00	14.58	0.20	4.77	9.64	3.17	0.79	0.48	99.45	0.3684	3.057	0.7135	3.960						
Katla	Lacasse et al 20	IC95-68	48.56	13.53	4.17	0.00	14.55	0.23	4.74	9.64	3.13	0.74	0.48	99.77	0.3674	3.070	0.7125	3.870						
Katla	Lacasse et al 20	IC95-66	48.97	13.42	4.30	0.00	14.41	0.25	4.54	9.32	3.21	0.81	0.53	99.76	0.3596	3.174	0.6945	4.020						

Figure C1: Process geochemical data from all four Katla data sets. Page 36 contains the first half of the data and page 37 the second portion.

						T Yang			Sugawara						
Ave P	1σ	P Range	D plag-Ol	P Ca	DP	T	1σ	Range	T	1σ	Range	Sample Number	Ave. Pressure		Kilometers
8.0431	1.2289	3.0841	1.2666	8.0904	-0.0473	1220.58	7.20	18.07	1118.22	3.80	9.53	1	6.0811		28.3009
8.6193	1.1201	3.1670	0.6730	8.0162	0.6030	1210.60	6.56	18.55	1110.27	3.46	9.79	2			30.32814
4.2226	0.6107	1.6774	0.3738	3.6969	0.5257	1171.62	3.58	9.83	1133.76	1.85	5.08	3			14.8577
5.0800	0.8507	2.3339	0.4852	4.1744	0.9056	1178.70	4.98	13.67	1113.39	2.61	7.15	4			17.87483
6.5634	1.0295	2.4003	1.1770	6.2955	0.2679	1197.03	6.03	14.06	1121.19	3.16	7.38	5			23.0943
5.0952	0.9889	2.5610	1.2433	5.1577	-0.0625	1196.87	5.79	15.00	1116.85	3.04	7.87	6			17.92832
5.0780	0.7754	1.9629	0.9238	4.5798	0.4982	1204.82	4.54	11.50	1123.89	2.38	6.02	7			17.86784
7.1897	0.9829	2.8143	0.6076	5.6260	1.5637	1213.21	5.76	16.49	1118.40	3.03	8.67	8			25.29815
6.6810	1.2269	3.5447	0.6774	4.5827	2.0983	1211.08	7.19	20.76	1115.77	3.78	10.93	9			23.50799
7.7755	1.1521	2.7706	1.4658	7.3866	0.3890	1223.57	6.75	16.23	1116.25	3.56	8.57	10			27.35935
6.0842	1.0568	3.0646	0.5437	4.0725	2.0117	1197.33	6.19	17.95	1113.57	3.25	9.44	11			21.40822
6.8734	1.0390	2.7238	0.9537	5.4345	1.4389	1213.26	6.09	15.96	1112.90	3.21	8.42	12			24.18503
6.4379	1.0666	2.7800	0.9970	5.1536	1.2843	1210.42	6.25	16.29	1112.64	3.29	8.59	13			22.65284
6.5902	0.9769	2.6214	0.8250	5.2757	1.3145	1209.61	5.72	15.36	1113.73	3.01	8.09	14			23.18861
6.9045	1.1287	2.8834	1.0779	5.8609	1.0436	1210.98	6.61	16.89	1109.74	3.49	8.92	15			24.29435
6.8799	1.1497	2.9361	1.1306	5.6772	1.2026	1214.34	6.74	17.20	1110.37	3.56	9.09	16			24.20782
6.8491	1.0824	2.8153	1.0123	5.6593	1.1898	1213.99	6.34	16.49	1111.44	3.35	8.71	17			24.09969
6.7309	1.0649	2.7251	0.9992	5.7147	1.0163	1211.40	6.24	15.96	1111.46	3.29	8.42	18			23.68379
6.1901	1.0692	2.5287	1.1929	5.2703	0.9198	1211.87	6.26	14.81	1112.31	3.30	7.81	19			21.78077
6.2457	0.9729	2.4060	0.9973	5.2387	1.0070	1211.65	5.70	14.09	1113.54	3.00	7.43	20			21.97641
1.2152	0.3698	1.0214	0.1368	-1.2419	2.4570	1139.21	2.17	5.98	1112.14	1.12	3.10	21			4.275718
6.8008	0.9439	2.3923	0.9175	5.7847	1.0162	1217.77	5.53	14.01	1119.99	2.91	7.37	22			23.92975
6.5440	0.9304	2.2918	0.9554	5.6087	0.9353	1216.22	5.45	13.43	1117.58	2.87	7.07	23			23.02597
5.1905	0.9162	2.7109	0.3414	3.0865	2.1040	1184.85	5.37	15.88	1113.18	2.81	8.32	24			18.2637
6.2458	0.8544	2.4634	0.4922	4.5017	1.7441	1199.38	5.00	14.43	1114.26	2.63	7.58	25			21.97665
6.1370	0.8547	2.4086	0.5862	4.6658	1.4712	1201.36	5.01	14.11	1115.48	2.63	7.41	26			21.59387
5.8746	0.7887	2.2624	0.4742	4.3400	1.5346	1198.00	4.62	13.25	1116.44	2.42	6.96	27			20.67071
5.8028	0.8243	2.2374	0.6611	4.4731	1.3297	1199.73	4.83	13.11	1112.77	2.54	6.89	28			20.41799
6.0974	0.8891	2.3097	0.8129	4.9876	1.1098	1206.33	5.21	13.53	1116.28	2.74	7.11	29			21.45471
6.7269	0.9087	2.3777	0.8288	5.4926	1.2343	1210.88	5.32	13.93	1113.68	2.81	7.34	30			23.66949
6.4968	0.9279	2.4470	0.8318	5.2277	1.2691	1210.71	5.44	14.33	1115.89	2.86	7.55	31			22.8599
6.0362	0.6788	1.9284	0.4365	4.4863	1.5498	1208.80	3.98	11.30	1121.03	2.09	5.93	32			21.2391
6.5722	0.8698	2.3423	0.7213	5.3188	1.2534	1208.38	5.10	13.72	1117.02	2.68	7.22	33			23.1252
6.3991	0.9506	2.4258	0.9115	5.2732	1.1259	1212.93	5.57	14.21	1117.72	2.93	7.47	34			22.51611
6.2454	0.8236	2.2577	0.6437	4.9232	1.3223	1208.77	4.82	13.23	1120.70	2.53	6.94	35			21.97552
6.5514	0.8617	2.2570	0.6989	5.5059	1.0454	1212.56	5.05	13.22	1120.07	2.65	6.95	36			23.05196
6.8127	0.9667	2.5625	0.8564	5.5251	1.2876	1213.79	5.66	15.01	1115.52	2.98	7.91	37			23.97149
6.0530	0.8085	2.1970	0.6303	4.7788	1.2742	1207.37	4.74	12.87	1118.94	2.49	6.76	38			21.29834
6.2655	0.8243	2.2523	0.6376	4.9234	1.3422	1208.37	4.83	13.19	1118.45	2.54	6.93	39			22.04611
7.0784	0.9135	2.4466	0.7346	5.8979	1.1805	1215.68	5.35	14.33	1118.76	2.82	7.54	40			24.90637
6.3527	0.8680	2.2365	0.7784	5.2954	1.0573	1209.02	5.08	13.10	1117.44	2.67	6.89	41			22.35278
6.9430	0.9177	2.3851	0.8371	5.8588	1.0842	1215.34	5.38	13.97	1118.05	2.83	7.35	42			24.42998
6.9234	1.0192	2.6313	0.9406	5.8925	1.0309	1213.09	5.97	15.41	1114.26	3.15	8.13	43			24.36095
7.0448	0.9566	2.5724	0.7930	5.8462	1.1986	1212.66	5.60	15.07	1116.15	2.95	7.94	44			24.78806
7.4235	0.9244	2.4065	0.7964	6.3906	1.0328	1216.13	5.41	14.10	1116.11	2.85	7.43	45			26.12061
6.9463	0.9998	2.4332	1.0333	6.1106	0.8357	1215.61	5.86	14.25	1114.34	3.09	7.52	46			24.44162
7.4870	1.0406	2.4444	1.1658	6.7633	0.7236	1219.25	6.10	14.32	1118.87	3.21	7.54	47			26.34403
6.6536	1.0355	2.4805	1.1356	5.9748	0.6787	1218.10	6.07	14.53	1118.81	3.19	7.65	48			23.41153
8.1960	1.1677	2.7128	1.4907	7.5854	0.6106	1227.85	6.84	15.89	1115.76	3.62	8.40	49			28.83877
7.7595	1.0808	2.5860	1.3297	7.2427	0.5168	1222.56	6.33	15.15	1118.24	3.34	7.99	50			27.30304
6.9937	1.1165	3.1083	0.6456	4.9767	2.0170	1201.11	6.54	18.21	1113.73	3.44	9.58	51			24.60845

Figure C2: Pressure and temperature calculations matching the data from page 36.

6.4346	0.9516	2.4683	0.8797	5.3477	1.0868	1203.69	5.57	14.46	1109.87	2.94	7.63		52			22.64102
7.6351	1.0399	2.5092	1.1234	6.7409	0.8942	1220.11	6.09	14.70	1112.89	3.22	7.77		53			26.86509
5.8943	0.9066	2.4169	0.7816	4.5427	1.3517	1202.73	5.31	14.16	1110.52	2.80	7.46		54			20.74012
6.4810	0.9241	2.2917	0.9383	5.4776	1.0034	1211.27	5.41	13.42	1115.35	2.85	7.07		55			22.80447
3.8585	0.7867	2.1893	0.5175	2.2810	1.5776	1172.07	4.61	12.83	1106.11	2.42	6.73		56			13.5768
6.3847	0.9877	2.3613	1.0578	5.4553	0.9294	1207.06	5.79	13.83	1108.80	3.05	7.30		57			22.46549
5.7672	0.8561	2.4631	0.4934	3.9569	1.8102	1197.26	5.02	14.43	1117.77	2.63	7.57		58			20.2926
6.4279	0.8907	2.2022	0.8992	5.4186	1.0093	1209.35	5.22	12.90	1113.93	2.75	6.79		59			22.61767
5.9882	0.9024	2.2910	0.8032	4.8951	1.0931	1206.27	5.29	13.42	1114.58	2.78	7.06		60			21.07033
5.6361	1.0161	2.4337	1.2192	4.8144	0.8218	1205.50	5.95	14.26	1105.61	3.14	7.53		61			19.83159
5.2322	0.9457	2.4363	0.8879	4.0620	1.1702	1191.29	5.54	14.27	1110.04	2.91	7.51		62			18.41036
6.3072	0.7969	1.9645	0.8137	5.2773	1.0298	1206.64	4.67	11.51	1117.03	2.45	6.05		63			22.19273
5.2639	0.6985	1.8416	0.5754	4.0924	1.1714	1195.42	4.09	10.79	1117.59	2.14	5.65		64			18.52168
5.9345	0.9430	2.2665	0.9854	5.0013	0.9332	1205.75	5.52	13.28	1114.42	2.91	6.99		65			20.88136
7.0717	0.8901	2.2162	0.9056	6.0532	1.0185	1215.70	5.21	12.98	1120.52	2.74	6.83		66			24.88274
6.6189	0.9287	2.2470	0.9637	5.7526	0.8663	1209.86	5.44	13.16	1117.44	2.86	6.92		67			23.28943
6.6958	0.7633	2.0104	0.6451	5.5451	1.1507	1210.57	4.47	11.78	1119.78	2.35	6.19		68			23.56027
6.4979	0.9141	2.2047	0.9118	5.6471	0.8508	1212.05	5.35	12.92	1117.02	2.82	6.80		69			22.86382
6.6203	0.8307	2.1089	0.7395	5.6604	0.9599	1210.55	4.87	12.35	1118.86	2.56	6.49		70			23.29467
6.3763	0.8241	2.0286	0.8437	5.3754	1.0009	1209.45	4.83	11.88	1117.13	2.54	6.25		71			22.43584
6.2462	0.8318	2.0542	0.8368	5.2575	0.9886	1208.13	4.87	12.03	1117.48	2.56	6.33		72			21.97811
6.3260	0.9194	2.2430	0.9319	5.3736	0.9524	1208.73	5.39	13.14	1113.80	2.84	6.92		73			22.25896
6.2362	0.7546	2.0329	0.6191	4.8853	1.3509	1207.73	4.42	11.91	1119.87	2.32	6.25		74			21.94299
6.3239	0.9082	2.2888	0.8807	5.2823	1.0416	1208.81	5.32	13.41	1115.35	2.80	7.06		75			22.25157
6.3345	0.8178	2.1048	0.7462	5.2479	1.0866	1209.00	4.79	12.33	1117.38	2.52	6.48		76			22.28895
5.3156	0.8607	2.1153	0.8067	4.3103	1.0053	1198.71	5.04	12.39	1110.59	2.65	6.52		77			18.70361
6.1997	0.9884	2.3586	1.0225	5.3497	0.8499	1209.18	5.79	13.82	1109.50	3.06	7.30		78			21.81443
6.3822	1.0242	2.3911	1.1885	5.5883	0.7939	1211.83	6.00	14.01	1112.41	3.17	7.39		79			22.45664
6.4045	1.2012	2.7623	1.4658	5.6140	0.7906	1207.38	7.04	16.18	1104.98	3.72	8.56		80			22.53532
6.8686	1.2611	2.9332	1.5491	6.2370	0.6316	1214.23	7.39	17.18	1108.81	3.91	9.09		81			24.16814
6.4257	1.0321	2.5527	1.0578	5.4318	0.9939	1208.18	6.05	14.95	1110.25	3.19	7.89		82			22.60994
6.2212	1.1087	2.6086	1.2724	5.3784	0.8428	1201.67	6.49	15.28	1112.42	3.42	8.05		83			21.89035
2.7204	0.6070	1.7743	0.1570	0.3636	2.3568	1151.87	3.56	10.39	1113.52	1.85	5.40		84			9.572094
5.2298	0.9189	2.6680	0.4310	3.1771	2.0527	1184.13	5.38	15.63	1112.82	2.82	8.19		85			18.40198
5.4907	1.0248	2.8551	0.7486	3.9608	1.5299	1191.08	6.00	16.73	1108.37	3.16	8.80		86			19.31998
5.6145	1.0689	2.8637	0.9218	4.2372	1.3774	1189.65	6.26	16.78	1106.71	3.30	8.84		87			19.75562
6.4648	1.1151	2.7177	1.2070	5.4578	1.0071	1203.83	6.53	15.92	1107.75	3.45	8.41		88			22.74739
7.0193	1.2544	2.8140	1.5409	6.2027	0.8165	1209.99	7.35	16.48	1110.84	3.88	8.71		89			24.69831
5.1323	0.7391	2.0630	0.5357	3.7408	1.3915	1194.40	4.33	12.09	1122.20	2.26	6.32		90			18.05889
4.8464	0.5635	1.4468	0.4292	3.7044	1.1420	1188.46	3.30	8.48	1115.22	1.73	4.44		91			17.05285
5.2675	0.5941	1.6570	0.3805	3.9454	1.3221	1192.62	3.48	9.71	1119.00	1.82	5.08		92			18.53443
4.7382	0.6837	1.9650	0.4088	3.0745	1.6637	1183.78	4.00	11.51	1114.93	2.10	6.03		93			16.67214
5.9895	0.6266	1.6556	0.4056	4.8586	1.1308	1193.90	3.67	9.70	1117.36	1.92	5.09		94			21.07483
6.7132	0.8205	2.0232	0.7326	5.8374	0.8758	1202.98	4.81	11.85	1112.49	2.53	6.24		95			23.6213
7.5269	1.0371	2.5228	1.0779	6.7236	0.8034	1213.99	6.08	14.78	1113.77	3.21	7.80		96			26.48463
7.7379	1.0859	2.7841	1.0551	6.4068	1.3312	1218.98	6.36	16.31	1116.45	3.35	8.60		97			27.22704
6.3689	0.9594	2.7222	0.5712	4.9698	1.3991	1204.90	5.62	15.95	1114.59	2.96	8.39		98			22.41
4.1493	0.7280	2.0877	0.4348	2.5358	1.6134	1176.04	4.26	12.23	1111.48	2.23	6.40		99			14.59984
6.7869	0.9621	2.4381	0.9175	5.8402	0.9467	1209.97	5.64	14.28	1113.88	2.97	7.53		100			23.88069
6.7978	0.9147	2.3600	0.8599	5.7285	1.0693	1208.62	5.36	13.82	1115.24	2.82	7.28		101			23.91903
6.3152	0.7583	2.1044	0.5580	5.0319	1.2833	1199.26	4.44	12.33	1116.11	2.33	6.48		102			22.22086
7.1275	1.2614	3.5805	0.8077	5.2157	1.9118	1216.77	7.39	20.97	1117.80	3.89	11.04		103			25.07918
5.3325	0.7089	1.9857	0.5061	3.9255	1.4070	1198.18	4.15	11.63	1122.33	2.17	6.08		104			18.7632
5.6403	0.6901	1.9781	0.4274	4.2141	1.4262	1198.86	4.04	11.59	1123.97	2.11	6.06		105			19.84612
5.7917	0.7111	2.0577	0.4052	4.3226	1.4691	1198.25	4.17	12.05	1119.01	2.18	6.32		106			20.379
6.1662	0.8254	2.2272	0.6871	4.9158	1.2504	1199.86	4.84	13.05	1114.23	2.54	6.86		107			21.6966
7.3576	1.1401	2.7431	1.1552	6.7715	0.5861	1212.89	6.68	16.07	1107.21	3.54	8.51		108			25.8888
5.5923	0.7195	1.9950	0.5202	4.2736	1.3187	1197.49	4.22	11.69	1119.47	2.21	6.12		109			19.6773
6.5432	0.7917	2.1955	0.5583	5.3565	1.1867	1201.21	4.64	12.86	1116.83	2.44	6.75		110			23.02314
4.6690	0.6511	1.8196	0.4669	3.1735	1.4955	1190.47	3.81	10.66	1115.41	2.00	5.59		111			16.42846
5.2314	0.6653	1.8726	0.4646	3.9528	1.2786	1195.83	3.90	10.97	1127.40	2.03	5.72		112			18.40756
5.6614	0.6847	1.6862	0.6129	4.5412	1.1202	1204.75	4.01	9.88	1115.58	2.11	5.19		113			19.92058
7.5866	0.9759	2.4413	1.1517	7.2367	0.3499	1222.70	5.72	14.30	1115.58	3.02	7.55		114			26.69457
6.2331	0.6693	1.7326	0.6080	5.1345	1.0986	1200.12	3.92	10.15	1118.94	2.06	5.33		115			21.93215
6.0090	0.6277	1.7842	0.4108	4.7066	1.3024	1197.99	3.68	10.45	1122.16	1.92	5.47		116			21.14359
5.4629	0.6447	1.8930	0.3095	3.8749	1.5880	1191.91	3.78	11.09	1119.51	1.98	5.80		117			19.22198
															Standard Deviation	3.53906

Figure C3: Pressure and temperature calculations for the second portion of the data found on page 37. Average depth is ~22 km with a 3.5 km standard deviation.